Journal of Geodesy (2001) 75: 469–490

Journal of Geodesy

GEOID99 and G99SSS: 1-arc-minute geoid models for the United States

D. A. Smith (✉), D. R. Roman

National Oceanic and Atmospheric Administration/National Geodetic Survey, 1315 East–West Highway, Silver Spring, MD 20910, USA, e-mails: dru.smith@noaa.gov, dan.roman@noaa.gov; Tel.: +1-301-713-3202; Fax: +1-301-713-4172

Received: 26 June 2000 / Accepted: 23 April 2001

Abstract. Two new geoid models have been computed for the United States and its territories. The first model is the purely gravimetric G99SSS model, approximating the geopotential surface $W_0 = 62636856.88\ m^2/s^2$ and referenced to the geocentric GRS-80 ellipsoid whose origin coincides with the ITRF96(1997.0) origin. The other model is the hybrid GEOID99 model, which encompasses all gravimetric information of G99SSS as well as the vertical datum information of 6169 GPS-derived NAD 83 (North American Datum 1983) ellipsoid heights co-located with spirit-leveled NAVD 88 (North American Vertical Datum 1988) Helmert orthometric heights. The coverage of both models in the conterminous United States (CONUS) is from 24°N to 58°N latitude and 230°E to 300°E longitude. Long-wavelength geoid structure was controlled by the EGM96 model coefficients, medium-scale information by 2.6 million gravity measurements, and local features through the use of 30-arc-second and (recently created) 3-arc-second digital elevation models. In addition to new elevation data, there were corrected errors in the old elevation data, better satellite altimetry data, and ellipsoidal corrections in G99SSS and GEOID99 that were not applied in G96SSS and GEOID96. The GEOID99 model replaces the GEOID96 model as the primary conversion surface between NAD 83 ellipsoid heights and NAVD 88 Helmert orthometric heights. While GEOID96 had the ability to convert absolute heights (of the 1996 GPS-on-bench-mark data set, or GPSBMs) at the ±5.3-cm level, GEOID99 works with the latest GPSBMs at the ±4.6-cm level. The improvement from 5.5 to 4.6 cm in RMS further translates into almost 2 cm of additional accuracy in single-tie differential GPS-based leveling over most short baselines. Of this 4.6 cm, some 2.0 to 2.5 cm is attributed to correlated errors in the gravimetric geoid and local GPS errors, decorrelating around 40 km. The GPS-derived ellipsoid heights in CONUS have changed since 1996 due to an increased number of observations and new adjustments of previously observed areas. This new GPS data is reflected in GEOID99, but not GEOID96, which effectively renders GEOID96 out of date (in an absolute sense), so that the absolute agreement between GEOID96 and the 1999 set of GPSBMs is only at the ±6.5-cm level. In addition to the geoid models in CONUS, gravimetric geoid models were produced in Alaska, Hawaii, and Puerto Rico and the American Virgin Islands. Surface deflection of the vertical models were also computed and show agreement with astro-geodetically determined deflections below the 1-arc-second level.

Key words: Geoid – GPS – Datums – Reference systems – Gravity – Deflections of the Vertical

1 Introduction

The demand for a highly accurate geoid model in the United States (US) has grown substantially in the last decade (Parks and Milbert 1995; Henning et al. 1998). In fact, with the success of GEOID96 (Smith and Milbert 1999), the demand became even greater for a similar geoid, but with increased accuracy. In order to move towards this goal, two new high-resolution geoid undulation models have been computed by the National Geodetic Survey (NGS) for the USA, G99SSS and GEOID99. The G99SSS model is a gravimetric, geocentric geoid undulation model, approximating the geopotential surface $W_0 = 62636856.88\ m^2/s^2$. This value of W_0 was chosen to comply with the work of Burša (1995). GEOID99 is a hybrid model, meaning that it incorporates both the gravimetric information of G99SSS as well as information obtained through GPS measurements on spirit-leveled bench marks. Like GEOID96 (Burša 1995), the GEOID99 model was built to support the direct conversion of NAD 83 (Schwarz 1989) ellipsoid heights into NAVD 88 (Zilkoski et al. 1992) Helmert orthometric heights.

In addition to customer demand for a better geoid model, there were substantial scientific reasons to compute a new model. Among these were the following: the creation of NGSDEM99, a new 1-arc-second digital

elevation model (DEM) for the northwest US (Smith and Roman in press); the completion of the high-accuracy reference networks, HARNs (Bodnar 1990; Doyle 1993; Flynn 1998; Strange and Love 1991) and first re-observations of the Federal base network vertical component, FBNVC (Frakes 1999); the acquisition of significant new gravity data; the correction of a 15×15-arc-second mis-registration error in the TOPO30 DEM (Row and Kozleski 1991); and a new method of computing the ellipsoidal corrections for Stokes' formula (Fei and Sideris 2000).

2 New data and theory

Improvements between the 1996 and 1999 NGS geoid models are primarily based on improved data sets with some new theory involved. New data sets include an updated 1-arc-second DEM for the northwest USA, a complete set of NAD 83 GPS height data on NAVD 88 leveled bench marks for all 48 conterminous United States (CONUS), and recently acquired gravity data sets (terrestrial, altimetric, and airborne).

Improvements to geoid computation theory and methodology include the use of multiple bands to minimize the convergence of the meridian error inherent in using a 2-D FFT (fast Fourier transform) for computing terrain corrections (TCs). (See also Kirby and Featherstone 1999.) Also, an improved method of computing the ellipsoidal corrections for Stokes' formula (Fei and Sideris 2000) was incorporated to more accurately solve the geodetic boundary-value problem in computing G99SSS.

2.1 New digital elevation model

DEMs are used to generate a grid of terrain corrections for the computation of Faye anomalies (see e.g. Smith and Milbert 1999). In GEOID96, a 30-arc-second interval grid, TOPO30 (Row and Kozleski 1991), was selected for the entire CONUS region. For GEOID99, a new 1-arc-second DEM, NGSDEM99 (Smith and Roman in press), was available. The NGSDEM99 model was built from 7.5-arc-minute quadrangles of the United States Geological Survey (USGS) and 'level 1' digital terrain elevation data (DTED) of the National Imagery and Mapping Agency (NIMA). It covers the northwest USA (39°–49°N, 234°–256°E). Further information is also available at http://www.ngs.noaa.gov/DEM.

Finally, a mis-registration of TOPO30, placing nearly all data southwest by 15×15 arc seconds, was found by the NGS in 1997. This was mostly correctable by shifting all data northeast by 15×15 arc seconds, creating a modified TOPO30 file for use in GEOID99. Unfortunately the error was not 100% consistent, making the use of the modified TOPO30 file acceptable, but still possibly containing some erroneously registered height values.

2.2 New GPS on leveled bench marks

In 1998, the NGS completed the HARN adjustments of the 48 CONUS. The completion of this network was a landmark achievement for the NGS, adding thousands of new GPS heights on leveled bench marks (GPSBMs) (Milbert 1998) to the 2951 used in the production of GEOID96 (Smith and Milbert 1999). The completion of the HARNs in 1998 was an opportunity to update the geoid model and use real data, not extrapolation (Smith and Milbert 1999), to model the local trends in the disagreement between the geoid and GPSBMs.

However, almost as soon as the HARN ended, the FBNVC began; first in Wisconsin, and then moving to Washington and Oregon. This effort is primarily a re-visiting of each of the 48 states to re-observe the old HARNs and to add some new survey points, but most especially to observe with such accuracy as to achieve ± 1-cm (1-σ) GPS-derived ellipsoid heights (Frakes submitted). However, only Wisconsin was observed, adjusted and formally part of the NGS integrated database (NGSIDB) by the deadline for inclusion in GEOID99. The Washington and Oregon data were observed and preliminarily adjusted and were used in GEOID99 before final adjustment and loading of the GPS data into the NGSIDB. Researchers at the NGS were confident that no significant difference between the preliminary and final adjustments of Washington and Oregon would be seen (Milbert and Pursell (NGS) personal communication). On 26 August 1999 the final GPSBM data set was chosen for use in GEOID99, containing 6169 GPSBMs. These points are plotted in Fig. 1.

The final criteria for selection of the 6169 points are described in an online NGS document (Smith and Roman 1999). Briefly, the criteria are as follows.

(1) A, B or first-order GPS data were used to determine the ellipsoid height.
(2) Leveling (of various orders and classes) was performed according to Federal Geodetic Control Subcommittee (FGCS) specifications and procedures to determine the orthometric height (see Federal Geodetic Control Committee (FGCC) 1984).
(3) All GPS and leveling data refer to NAD 83 or NAVD 88, respectively.

Although 6341 points fulfilled these criteria, this was reduced to 6169 though the detection and rejection of outliers (Smith and Roman 1999). Of the 6169 points, a tally for each combination of GPS order and leveling order is shown in Table 1.

The most numerous bench marks are from the *most* accurate leveling (first-order), while the most numerous GPS is the *least* accurate (again, called first-order). Although there were many first-order (leveling) bench marks the *full set* of bench marks was utilized in GEOID99 to make that model useful to users of all orders of bench marks.

Between 1996 and 1999 new GPSBMs were added and some old ones were re-observed, re-adjusted, or had errors detected and repaired. This change from one value of h (or H) in 1996 to a new value in 1999 will have a direct impact on the hybrid geoid model. There were 2819 points that were common to both GPSBM data sets for both GEOID96 and GEOID99, and were not

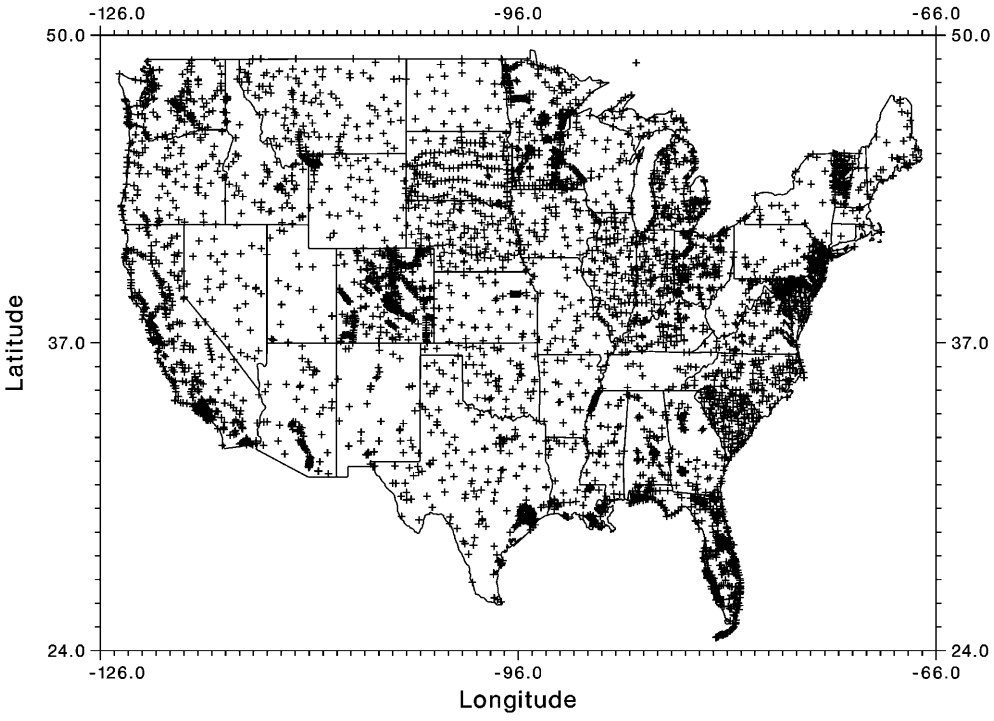

Fig. 1. Distribution of the final 6169 GPS bench marks used in GEOID99

Table 1. Breakdown of 6169 GPSBMs by GPS order and leveling order

	A-order GPS	B-order GPS	First-order GPS	Totals
Unknown-order leveling	93	30	2	125
First-order leveling	195	1290	1777	3262
Second-order leveling	83	735	1128	1946
Third-order leveling	5	212	619	836
Totals	376	2267	3526	6169

Table 2. Count of total, retained and rejected GPSBM points for both the GEOID96 and GEOID99 models

	Rejected in GEOID96	Retained in GEOID96	Not in GEOID96	Total
Rejected in GEOID99	47	83	116	246
Retained in GEOID99	73	2819	3277	6169
Not in GEOID99	5	49	–	–
Total	125	2951	–	–

Table 3. Statistics of changes in h and H from 1996 to 1999 (m)

	No. of points	Max	Min	Average	σ
All h values	2819	0.271	−0.288	−0.005	±0.042
Only changed h values	548	0.271	−0.288	−0.024	±0.094
All H values	2819	0.146	−0.071	0.000	±0.004
Only changed H values	81	0.146	−0.071	0.000	±0.022

rejected as outliers. The relationship of the total, retained, and rejected points for both models are summarized in Table 2.

Most of the common points were unchanged, although 522 changed in latitude, 524 changed in longitude, 548 changed in ellipsoid height and, of these, 471 changed in all three directions. Only 81 points had any change in orthometric height. This shows the dynamic nature of the GPSBM data set, predominantly in the ellipsoid height component, due to re-observations and re-adjustments of the GPS data. In Table 3, statistics are given for all points but also for only those points that experienced some change.

From Table 3, clearly the changes in the ellipsoid heights are more profound than those in the orthometric heights. The extent of these changes in orthometric height is also very localized compared to the effects of the ellipsoid height changes. In Fig. 2, the ellipsoid height changes are gridded at 30-arc-minute intervals to emphasize regional features rather than high-frequency local changes. Thus, one can clearly make out regional features in the Pacific northwest (PNW) ($42° \leq \phi \leq 49°$N, $235° \leq \lambda \leq 242°$E) and near Lake Michigan ($\phi = 45°$N, $\lambda = 271°$E). These are the locations of the FBNVC in Washington, Oregon, and Wisconsin. In addition, the New England area ($\phi = 43°$N, $\lambda = 288°$E) shows a large change, which is reflective of a combined re-adjustment of the HARNs in that area.

There are certainly some very *localized* changes in the ellipsoid heights as well. Locally, changes in ellipsoid heights at one point lead to changes in the ellipsoidal height difference between points [$\Delta(\Delta h)$] which, when compared to the distance separating the points, yield changes in the ellipsoid height gradient [$\Delta(\nabla h) = \Delta(\Delta h)$/distance] exceeding 2000 ppm. Of 473 pairs of ellipsoid

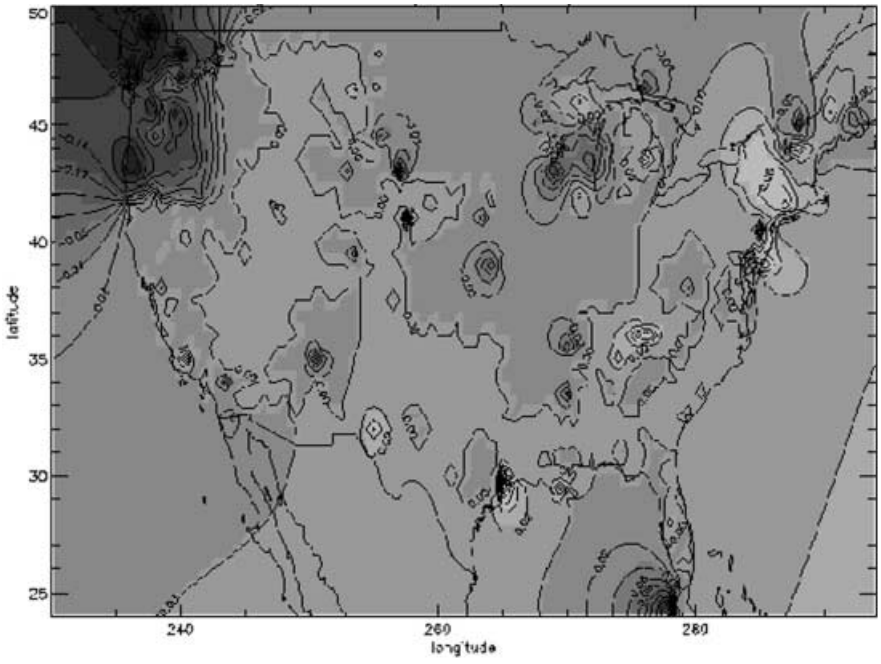

Fig. 2. Regional changes in the definition of NAD 83 ellipsoid heights between 1996 and 1999 (Contour Interval = 2 cm)

heights, the ellipsoid height gradient changes between neighboring points (separated by less than 1-arc-minute in both latitude and longitude) averaged 66.2 ± 218.5 ppm with a maximum of 2293.6 ppm. Of these 473 pairs, 81 had $\Delta(\nabla h) > 100$ ppm while 320 had $\Delta(\nabla h) = 0$ ppm. The maximum $\Delta(\nabla h)$ value of 2293.6 ppm is for a pair of points in Texas separated by 48 m where the Δh from 1996 to 1999 was +1 cm for one point and −10 cm for the other (note that only 20 ppm of the 2293.6 ppm can be attributed to round-off errors of ±0.5 mm for each coordinate). This level of height change is approximately at the noise level for which GPSBM data sets were cleaned (Milbert 1998; Smith and Milbert 1999; Smith and Roman 1999) and therefore it is understandable how these two points were retained in both the 1996 and 1999 GPSBM data sets.

2.3 Other new data

2.3.1 New gravity

Approximately 800 000 more gravity data points were used in GEOID99 than in GEOID96. Most of these were simply due to expanding the computational area for GEOID99 (from $24° \leq \phi \leq 53°$N, $230° \leq \lambda \leq 294°$E in GEOID96 up to $24° \leq \phi \leq 58°$N, $230° \leq \lambda \leq 300°$E for GEOID99). In addition to these measurements, 122 050 further measurements, located just offshore along the Gulf of Mexico (GOMEX) coastline were made available by Dr. Carlos Aiken (University of Texas at Dallas). These data were analyzed to determine their impact on the geoid. Gravimetric geoids were generated both with and without these data, and also both with altimeter-implied free-air gravity anomalies (FAGA) overlapping the region of these data and not overlapping (a total of four geoids). The method of computation was identical to that of computing G96SSS (Smith and Milbert 1999). The addition of the offshore data caused a slight increase in the residuals between interpolated geoid heights and GPSBM data (up from 17.9 cm without the new offshore data to 18.0 cm with these data). This level of change is very nominal and may result from interference between the altimetry and the GOMEX data. However, in a second analysis, where altimetry was not permitted to overlap with the GOMEX data, there was again a slight degradation of the agreement between gravimetric geoid and GPSBMs when the GOMEX data were used. As such, the new GOMEX data were kept out of GEOID99 until a more detailed analysis can be made.

2.3.2 Altimeter-implied free-air gravity anomalies

Two of the most recent FAGA data sets were analyzed to determine which would be best suited for use in GEOID99. Sandwell and Smith's version 9.2 (SS92), Smith (NOAA National Oceanic and Atmospheric Administration), personal communication; available online at http://topex.ucsd.edu and the Danish National Cadastre's (KMS's) 1998 anomalies (KMS98) (Andersen and Knudsen 1998) were incorporated with the terrestrial gravity data sets of the NGS to generate two separate experimental geoids. Incorporating these data sets consisted of concatenating them all into one file where they were treated the same thereafter (i.e. no weighting schemes were employed). After comparing the results of these two geoids, the KMS98 data were found to generate marginally better results than the SS92 data and were selected for continued use in the deep-ocean offshore regions. This preference for KMS FAGA products was also seen in previous NGS geoid studies (Smith 1997; Smith and Small 1999), because their data were least likely to contain OC 7 SST, a sea surface topography signal, aliased into the gravity field.

There were four major regions where GEOID99 computations were made: CONUS, Alaska, Hawaii, and

Puerto Rico and the US Virgin Islands (PR/VI). For each of these regions, it was necessary to determine the optimal combination of distance from shore and depth to create a land-mask filter to remove suspect, near-shore altimeter-implied FAGAs. The values selected to create the filters in the four regions are given in Table 4. These values were found empirically after numerous experimental geoids were computed and analyzed by comparison with GPSBM data.

The sole exception was for the extensive shallow reef in the Bahamas region, southeast of CONUS, where a supplemental filter (−1 m depth, 0 km from shore) was used to retain as much altimetry as possible in the Bahamas, as was the case for GEOID96 in the same region (Smith et al. submitted).

In the near-shore or shallow environments, the altimeter-implied FAGA were mostly eliminated, leaving only ship track data (which is largely the same ship track data used to generate GEOID96) to resolve features in the gravimetric field. To supplement these data, airborne surveys in the Florida and Bahamas regions were examined.

2.3.3 Airborne gravity surveys in Florida and the Bahamas

Two airborne gravity surveys were available over the Bahamas and south-central Florida from the NIMA. Previous errors in the storage of these data in both the NIMA and NGS databases caused them to be excluded from GEOID96. These errors were identified and fixed in 1997 by Bob Moose (NGS, personal communication). The results of a previous study (Smith et al. submitted) were re-examined, and it was decided not to incorporate these data into GEOID99.

2.4 New ellipsoidal corrections

Fei and Sideris (2000) have developed an algorithm to generate a grid to correct for the spherical approximations inherent in computing a gravimetric geoid through Stokes' solution to the third boundary value problem of physical geodesy (Heiskanen and Moritz 1967, p. 36). The basic premise is to generate a preliminary geoid using the spherical Stokes integral, and then use that preliminary grid in the computation of ellipsoidal corrections which, when added to the preliminary geoid, yield a final geoid model. Initial comparisons of experimental gravimetric geoids with and without this correction to GPSBMs indicated that the procedure does yield less north–south tilt in the residuals. This is an improvement to the gravimetric geoid, under the assumption that there is no significant north–south tilt in NAVD 88 or the GPS data. This procedure was thus adopted for G99SSS.

Table 4. Altimetry selection criteria for four computational regions

Region	Offshore buffer		Minimum depth (m)
	Arc minutes	km	
CONUS[a]	15	28	500
Alaska	10	19	0
Hawaii	30	55	3000
PR/VI	6	11	0

[a] For the Bahamas region, a 0-km offshore buffer and a 1-m minimum depth were used

3 Initial computations, tests and problems

In addition to testing the input data sets, various experimental geoids were computed to identify the best computational methods for producing GEOID99. For example, in constructing GEOID96, mean elevations on one 30-arc-second grid for the entire CONUS region were used to generate a grid of TCs using a 2-D FFT. The use of just a single grid was compared to results generated from multiple latitudinal bands in order to analyze the impact of the convergence of the meridian on the TCs. Additionally, the selection of a 2- or 1-arc-minute grid interval for the output GEOID99 grid interval was examined in the PNW region. Finally, at least a short-term provisional repair of the GTOPO30 DEM in Quebec, Canada needed to be created.

3.1 Single-run FFT TC vs multi-band

The decision to use multiple bands for estimating the terrain corrections was driven by experiments which showed large north–south TC errors when using the 2-D FFT with spherical distance computation (Strang van Hees 1990; Smith and Milbert 1999). In the PNW, a 3-arc-second version of NGSDEM99 was used for computing TCs using the standard $\rho = 2670$ kg/m^3, and to perform the computation the region was divided into 10 overlapping sub-grids. The number of sub-grids was determined from RAM limitations and initial analysis indicating how large an overlap region was needed to control 2-D FFT TC errors. Once terrain corrections were computed at the 3-arc-second interval (and tapering/padding of zeros were removed), there were 10 TC sub-grids which overlapped by 2° in latitude and longitude. These core-area sub-grids were then linearly merged, whereby the distance of a node from the edge of an overlapped region was used for a weight. The computed difference between the sub-grids in the north–south overlapped regions revealed that significantly different predictions were caused by the convergence of the meridians (as high as 31.3 mGal, but most with less than 0.5 mGal). However, the east–west overlap regions show almost no disagreements, further emphasizing that the convergence of the meridians is the primary cause of the disagreements. See Tables 5 and 6 for details.

The determination of the 3-arc-second TCs from DEM data in the PNW demonstrated that significant mismatches resulted from latitudinal bandwidths of 600–700 km. The significance of the disagreements that occurred in the overlapped portions (primarily between north–south sub-grid pairs) indicated that a multi-band approach should also be taken for the computation of terrain corrections at the 30-arc-minute level for all other large north–south regions (CONUS, and Alaska).

Hence for the CONUS (for use outside of the PNW), three bands of 30-arc-minute TCs were generated with 50% latitudinal overlap (1900 km). These three bands were linearly merged to reduce disagreement in the overlap regions. By accounting for the convergence of the meridians in the multi-band approach, the G99SSS reduces part of the north–south tilt errors that were in G96SSS. The disagreement between this three-band method and a single-run, 2-D FFT method (Smith and Milbert 1999) at 22 223 361 grid points has an average of 0.062 ± 0.835 mGal, with extremes of −57.363 and +74.569 mGal. In Alaska, the higher latitude magnifies the problem of meridian convergence. As such, seven bands were used to compute the Alaska TCs, each with 500 km north–south and overlapping 40% (200 km) with each neighboring band. For Hawaii and PR/VI the computational area was small enough to ignore the convergence of the meridians.

3.2 Two-arc-minute vs 1-arc-minute experiment

The GEOID96 model was produced on a 2-arc-minute grid. Recent results (Kotsakis and Sideris 1999) indicate that >1 cm structure in the geoid may be omitted if a grid spacing larger than 1-arc-minute is used (results were for Canada). The actual gravity coverage in most parts of the world is not at the 1-arc-minute spacing. However, it is not the gravity coverage, but the DEM (in this case at the 3-arc-second spacing in the PNW and 30-arc-second spacing elsewhere) which contributes most toward the high-frequency component of the geoid. This is due to both the incorporation of terrain corrections and the restoration of the Bouguer plate (Smith and Milbert 1999). Therefore, it is reasonable to assume that some level of omission error is being made between 1- and 2-arc-minute solutions. Additionally, commission error will be increased during interpolation in the 2-arc-second case over that in the 1-arc-second case.

To test this hypothesis in the US, the FBNVC ellipsoid heights in the states of Washington and Oregon were compared against preliminary 2- and 1-arc-minute geoid models. Because the GPS heights on the FBNVC points have a formal accuracy of 1 cm (1σ), they were the best data set for attempting to identify such a small omission error in the geoid. However, the points chosen were of mixed leveling orders and classes. This was because the FBNVC data in Washington and Oregon were preliminary data, and not yet loaded into the NGSIDB, and therefore full information (such as order of leveling) was not available for this study. Still, over the area of this study, it is believed that leveling errors (even at third order) will be small enough to have minimal impact. A final set of 104 GPSBMs (FBNVC) in Washington and Oregon were then compared to the preliminary geoid models. The average offset and standard deviations are 88.8 ± 17.1 cm for the 2-arc-minute geoid and 87.8 ± 16.6 cm for the 1-arc-minute geoid. This means that a slightly smaller (0.5-cm) RMS about the mean offset can be achieved due to the 1-arc-minute grid spacing. This impact is considered too large to be ignored, and therefore the computation of G99SSS and GEOID99 was chosen to be on a 1-arc-minute grid.

3.3 Difficulties with the Quebec DEM

In order to provide a larger overlap region with Canada (useful when comparing US and Canadian geoid models), it was decided to extend the computational area of GEOID99 north to 61° (to reduce edge effects, the final released area was limited to 58°). Gravity data existed in the NGS database for this region of Canada, but to extend the DEM northward required using either

Table 5. North minus south 3-arc-second TC differences between overlapping 2-D FFT regions in the Pacific northwest (mGal)

Name	Area (1,1) − area (2,1)	Area (1,2) − area (2,2)	Area (1,3) − area (2,3)	Area (1,4) − area (2,4)	Area (1,5) − area (2,5)
Latitude	43–45	43–45	43–45	43–45	43–45
Longitude	234–240	238–244	242–248	246–252	250–256
Minimum	−0.048	−0.113	−0.095	0.043	−0.007
Maximum	31.275	19.026	10.211	14.359	11.622
Average	0.203	0.204	0.428	0.439	0.282
Standard deviation	±0.279	±0.245	±0.444	±0.491	±0.418
RMS	0.345	0.319	0.617	0.659	0.504

Table 6. West minus east 3-arc-second TC differences between overlapping 2-D FFT regions in the Pacific northwest (mGal)

Name	(1,1) − (1,2)	(1,2) − (1,3)	(1,3) − (1,4)	(1,4) − (1,5)	(2,1) − (2,2)	(2,2) − (2,3)	(2,3) − (2,4)	(2,4) − (2,5)
Latitude	43–49	43–49	43–49	43–49	39–45	39–45	39–45	39–45
Longitude	122–120	118–116	114–112	110–108	122–120	118–116	114–112	110–108
Minimum	−0.088	−0.083	−0.179	−0.301	−0.240	−0.203	−0.138	−0.262
Maximum	0.179	0.188	0.188	0.104	0.236	0.310	0.249	0.188
Average	0.018	−0.005	−0.001	−0.017	0.022	0.061	0.015	−0.016
Standard deviation	±0.036	±0.027	±0.040	±0.059	±0.043	±0.063	±0.037	±0.062
RMS	0.040	0.027	0.040	0.061	0.048	0.087	0.040	0.064

GTOPO30 (USGS 1997) or GLOBE 1.0 (Hastings and Dunbar 1999), the only two readily available 30-arc-second DEMs for this area. It was imperative to have a good DEM in this region, as the TCs stored with the gravity points were all set at zero (which is far from the truth in this region) when NGS acquired them from Canada. Initial tests indicated that the DEM-based TCs were reasonable using either GTOPO30 or GLOBE, but the DEMs themselves both had an overall systematic bias of about 20 m relative to gravity observation point heights in the database. Because point heights are used to remove the Bouguer plate attraction, and DEM heights are used to restore that attraction (Smith and Milbert 1999), this discrepancy caused a large 'dip' in the geoid, pulling the entire northeast corner down by over 1 m. This subsequently caused a SW/NE geoid tilt across most of the eastern CONUS. Discussions with the National Geophysical Data Center (NGDC) (Hastings, personal communication), indicated that both GTOPO30 and GLOBE 1.0, and even DTED level 0 (NIMA), will be nearly identical in that region, as they all rely on Digital Chart of the World (DCW) maps.

One other DEM, JGP95E (Lemoine et al. 1998), a 5-arc-minute model, was tested for Quebec. In this test, the TCs were too low when compared to those of GTOPO30 (as expected from such a coarse model), but surprisingly the overall agreement between point heights and JGP95E showed less systematic disagreement than any previously tested DEM. Therefore, a 2-arc-minute densification of JGP95E was created for use solely for the computation of Bouguer plate terms, while the high-frequency component of GTOPO30 controlled the TCs. This mixing of DEMs almost completely removed the geoid tilts in Quebec.

4 Computation of G99SSS

Through the analysis of the above data sets, large portions of the computation of G99SSS were already done. The procedure is identical to that for G96SSS (Smith and Milbert 1999), except for some exceptions noted below for the CONUS, Alaska, Hawaii, and PR/VI regions.

4.1 Conus

TCs were derived from a 3-arc-second DEM in the PNW, 30-arc-second TOPO30 data elsewhere in the CONUS region, and the mixed JGP95E/GTOPO30 DEM for the Quebec region in multi-latitudinal bands. These data, together with the Bouguer correction and normal gravity gradient free-air correction (Heiskanen and Moritz 1967, p. 132) and the GRS-80 normal gravity formula, were applied to 2.6 million point surface gravity data to generate refined Bouguer anomalies (Δg_{RB})

$$\Delta g_{\mathrm{RB}} = g_{\mathrm{P}} - F + TC - A_B - \gamma_Q$$

where: g_{P} = measured gravity at P above geoid

F = free-air reduction from P to the

TC = terrain correction

A_B = attraction of Bouguer plate

γ_Q = normal gravity at point Q on the ellipsoid (1)

These refined Bouguer anomalies were then gridded using splines in tension, and the average 1-arc-minute DEM used to restore the Bouguer plate (Smith and Milbert 1999). This gave a 1-arc-minute grid of Faye anomalies (Moritz 1980, p. 419), which are used as an approximation of Helmert anomalies (Δg_{H})

$$\Delta g_H \approx \Delta g_{Faye} = g_P - F + TC - \gamma_Q \quad (2)$$

Following a similar procedure to Smith and Milbert (1999), the EGM96 model (Lemoine et al. 1998) was next used to compute a 1-arc-minute grid of gravity anomalies and geoid undulations 'in the masses' (as per Smith and Milbert 1999, Appendix), including the computation of a degree-zero term as per Smith (1998)

$$T_{2-360} = \frac{GM_1}{r}\sum_{n=2}^{360}\left(\frac{a_1}{r}\right)^n \sum_{m=0}^{n}\left[\left(\bar{C}_{nm} - \left(\frac{GM_2}{GM_1}\right)\left(\frac{a_2}{a_1}\right)^n \bar{C}^*_{nm}\right)\cos(m\lambda) + \bar{S}_{nm}\sin(m\lambda)\right]\bar{P}_{nm}(\cos\theta)$$

$$\Delta g_{0-360} = \Delta g_0 - \frac{\partial T_{2-360}}{\partial r} - \frac{2}{r}T_{2-360}$$

$$N_{0-360} = N_0 + \frac{1}{\gamma_Q}T_{2-360}$$

where: GM_1 = EGM96 value = $398600441.5 \times 10^6 \mathrm{m^3 s^{-2}}$

M_2 = GRS-80 value = $398600500.0 \times 10^6 \mathrm{m^3 s^{-2}}$

a_1 = EGM96 scale factor = 6378136.3m

a_2 = GRS-80 equatorial radius = 6378137.0m (3)

and where the N_0 and Δg_0 terms are computed from the following formulas (Heiskanen and Moritz 1967, pp. 101–102):

$$\Delta g_0 = \frac{1}{R}(GM_1 - GM_2) + \frac{2}{R}(W_0 - U_0)$$

$$N_0 = \frac{(GM_1 - GM_2)}{R\gamma_Q} - \frac{(W_0 - U_0)}{\gamma_Q}$$

where: R = Mean earth radius = 6371 km20

γ_Q = normal gravity at a point

W_0 = Current best estimate(Bursa 1995)

$= 62,636,856.88\ \mathrm{m^2 s^{-2}}$

U_0 = GRS-80 value = $62,636,860.85\ \mathrm{m^2 s^{-2}}$ (4)

As per Smith and Milbert (1999, Appendix), these EGM96 grids are used in a 'remove–compute–restore' technique to create residual Faye anomalies

$$\Delta g^{\mathrm{res}}_{\mathrm{faye}} = \Delta g_{\mathrm{Faye}} - \Delta g_{0-360} \quad (5)$$

A spherical approximation of the Stokes integral was used to convert residual Faye anomalies into residual co-geoid undulations for the CONUS region using the 1-D FFT approach (Haagmans et al. 1993; Smith and Milbert 1999)

$$N_{co}^{res} = \frac{R}{4\pi\gamma} \iint_{\sigma} \Delta g_{Faye}^{res} S(\psi) d\sigma \tag{6}$$

Addition of this residual co-geoid to the reference EGM96 geoid grid [Eq. (3)], and applying the first-order indirect effect (Smith and Milbert 1999), resulted in a preliminary gravimetric geoid model (designated case19) for the CONUS region

$$N = N_{co}^{res} + N_{0-360} + \delta N_1 \tag{7}$$

where the quadratic approximation of the primary indirect effect is

$$\delta N_1 = -\frac{\pi G \rho H^2}{\gamma} \tag{8}$$

In order to generate the final G99SSS model, ellipsoidal corrections were applied to the case19 preliminary geoid. Because the ellipsoidal corrections of Fei and Sideris (2000) are predominantly long-wavelength and computationally intensive, the 1-arc-minute case19 preliminary geoid was decimated to 1° and provided to Fei and Sideris (personal communication) so they could compute the ellipsoid corrections. These corrections were provided back to NGS on a 1° grid (shown in Fig. 3). The corrections were then densified to 1-arc-minute and added to the preliminary case19 model to generate the final G99SSS model.

In comparing G99SSS to G96SSS, the primary differences arise from the treatment of topography in the PNW, and the new altimetry data set. This is exemplified in Fig. 4.

4.2 Alaska, Hawaii, PR/VI

Similar steps were followed for these regions as for the CONUS region. TCs were derived from 3-arc-second DEMs for Hawaii and PR/VI, while a 30×60-arc-second DEM was used in Alaska (time and data constraints prohibited using finer data in Alaska). Geoid computations were again made on 1-arc-minute grids. Altimetry coverage was derived from the KMS98 data using the land-mask filters listed in Table 4 for each region. Because of a lack of good, densely spaced GPS on leveled bench marks in these regions, no hybrid geoid model was produced for them, and the final gravimetric geoid model was given the designation GEOID99.

5 Comparison of G99SSS to GPS heights on leveled bench marks

Comparison of the CONUS G99SSS grid with a sufficient GPSBM data set (Sect. 2.2) provides a means of estimating, and removing, possible systematic error sources in the geoid model, leveling, or GPS measurements. Components of this error that are modeled relate to a national bias and tilt and state-by-state biases, which have significant features at about the 400-km wavelength. With these errors modeled, a conversion surface to the G99SSS model generates the GEOID99 model for the direct transformation from GPS-derived NAD 83 heights at epoch 1986 [NAD 83(86)] to NAVD 88 orthometric heights.

As can be seen in Fig. 1, the density of the 6169 GPSBM data points is not uniform but does provide adequate coverage for reducing the initial errors if they are long wavelength in nature, as is expected of the signal generated by the state-by-state biases.

5.1 Reference frames

The computation of G99SSS included efforts to make this geoid model refer to the 'geocentric' GRS-80 ellipsoid. These efforts included the following.

(1) Using EGM96 to control the global geoid signal. The EGM96 geopotential model refers to the WGS-84 (G873) origin which is "... considered to be co-incident with the ITRF94 to better than 2 cm" (Lemoine et al. 1998, p. 11–4), where ITRF is the International Terrestral Reference Frame. In addition, the definition of the ITRF96 origin was done in such a way as to "... be the same as ... ITRF94" (Sillard et al. 1998, p. 3225).
(2) Transforming the latitude and longitude of gravity measurements from NAD 27 into NAD 83 [using the NGS NADCON software (Dewhurst 1990)], and further transforming them from NAD 83 into ITRF96(1997.0), using a seven-parameter transformation (Snay 1999) shown in Table 7, which is generally good to ± 1.3 cm (Smith and Milbert 1999).

Considering these issues, one may conclude that the origin of G99SSS is co-incident with ITRF96(1997.0) to better than 2 cm.

When the adoption of ITRF97(1997.0) was made in August 1999, the IERS declared that no transformation existed between the origin of ITRF96(1997.0) and that of ITRF97(1997.0). However, recent computations at the International GPS Service (IGS) indicate that a slight transformation may exist – about 1.5 cm along the Z-axis (Milbert and Snay (NGS), personal communication). The NGS is planning on adopting this transformation when computing ITRF97(1997.0) coordinates. Since a 1.5-cm transformation is no more significant than the 2-cm agreement between ITRF94(1996.0) and WGS84 (G873), the origin of G99SSS might be argued as ITRF97(1997.0) with as much confidence that it is claimed to be ITRF96(1997.0). However, this statement will be avoided for one major reason: the geocentric reference frame to which the gravity (and thus geoid) refers should be the same geocentric reference frame to which the GPS heights refer (see next section). And while transforming

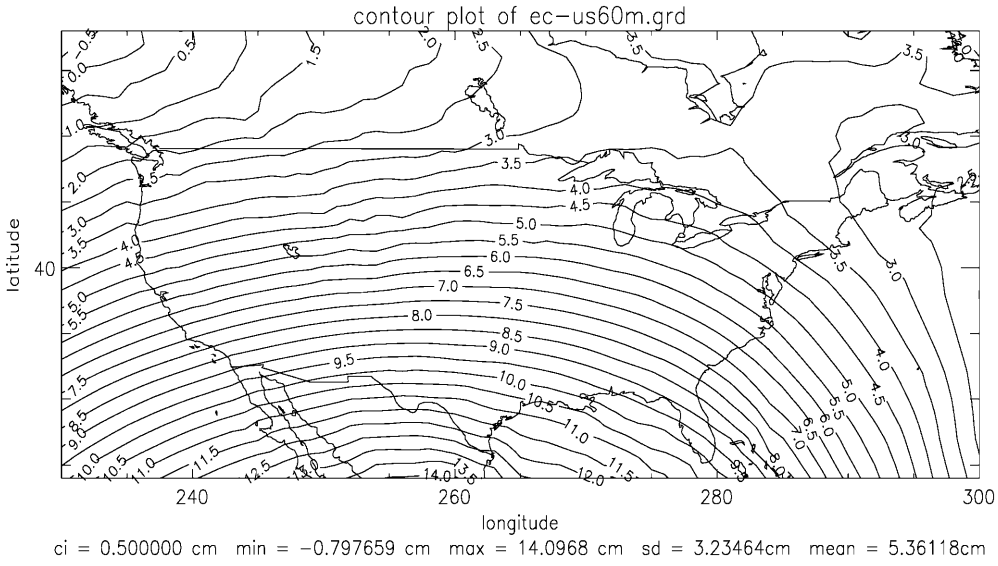

Fig. 3. 'Ellipsoid corrections' to the spherical Stokes integral over the CONUS (C.I. = 0.5 cm)

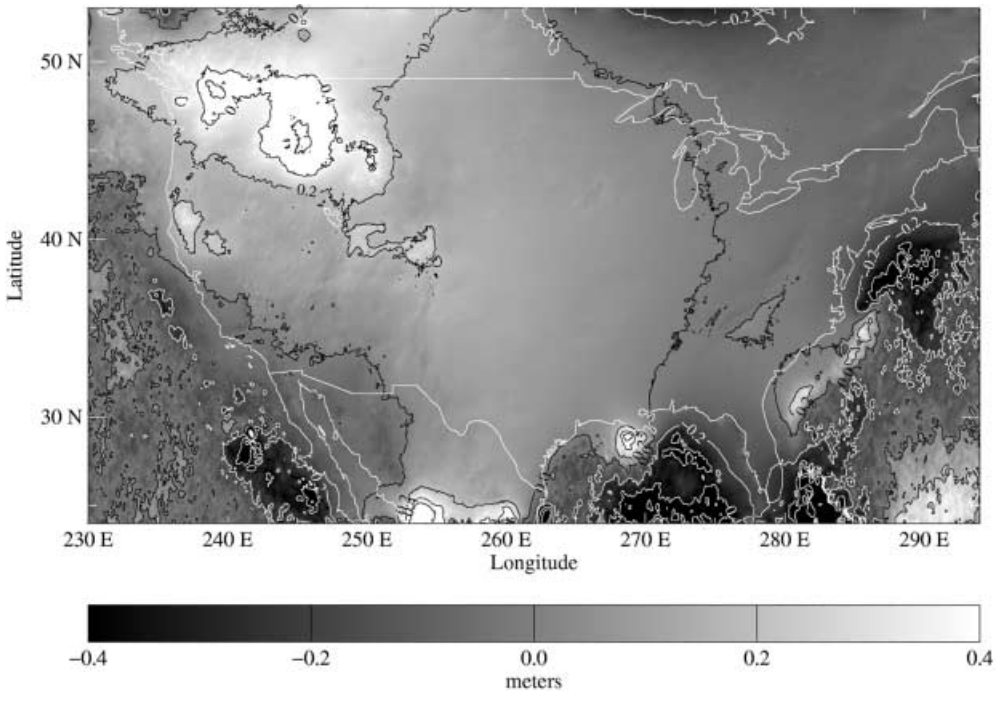

Fig. 4. Differences between G99SSS and G96SSS

Table 7. Seven-parameter transformation from NAD 83(86) to ITRF96(1997.0)

Δx	+0.9910 m
Δy	−1.9072 m
Δz	−0.5129 m
ω_x	12 503.3 × 10^{-11} radians
ω_y	4678.5 × 10^{-11} radians
ω_z	5652.9 × 10^{-11} radians
Scale	0.00 ppm

a gravity measurement by 1.5 cm is insignificant in relation to the observation errors, the transformation of GPS heights at the 1.5-cm level is very significant. As such, the origin of G99SSS will be considered to be the origin of ITRF96(1997.0).

5.2 The covariance function

Once G99SSS was computed, it was compared (using biquadratic interpolation) to the 6169 GPSBM data set (see Fig. 1). In order to have datum consistency, the G99SSS model was transformed from the ITRF96(1997.0) reference frame to NAD 83(86) using the seven-parameter transformation shown in Table 7 (Snay 1999). Transformation of the GPS heights from NAD 83(86) into the ITRF96/GRS-80 reference frame, similar to Smith and Milbert (1999), would achieve the same basic purpose of datum consistency.

The ellipsoid used in the creation of G99SSS was GRS-80, which is identical to that used in NAD 83(86). Therefore, no ellipsoid parameter changes needed to be applied when referring G99SSS to NAD 83(86). This

modified version of G99SSS will be referred to as G99SSS(NAD 83). Once the geoid model was transformed, then the comparison was made. The residuals, e, are computed as

$$e = N - (h - H) \tag{9}$$

where N is the G99SSS(NAD 83) geoid height, H is the NAVD 88 leveled Helmert orthometric height and h is the NAD 83(86) GPS-derived ellipsoid height.

The residuals, e, had an average of $+51.7$ cm, and a standard deviation of ± 21.7 cm. These statistics should be compared to those of G96SSS (Smith and Milbert 1999), where the average residual was $+31.4$ [after correcting an erroneous 12-cm bias (Smith and Milbert 1999)], and the standard deviation ± 15.6 cm. Much of the change in the standard deviation is due to the addition of new HARNs since 1996. This is discussed in further detail in Sect. 5.3. The change in the average is due to many factors, including the new method of computing TCs, the expanded computational area, and the change to KMS98 altimetry.

In the manner of GEOID96 (Smith and Milbert 1999), LS collocation was used to model the residuals between the gravimetric geoid (N) signal and the GPSBM ($h - H$) signal. Since collocation requires centered data, the average residual (i.e. 51.7 cm), as well as a trend surface, were first removed from the residuals. The trend surface was 0.15 ppm at an azimuth of 327°. This can be compared to the trend surface of G96SSS (0.06 ppm, 178° azimuth), and again the difference is due to new GPSBMs and finer terrain corrections in the PNW. The residuals were collected into 'bins' of 50 km and an empirical covariance function (ECV) was computed. A Gaussian covariance function (GCV) is then fitted to the ECV, where the GCV can be written

$$C_e(\psi) = C_{o,e} \exp[-(\psi/\xi_e)^2] \tag{10}$$

where ψ is the spherical separation between points, and $C_{0,e}$ and ξ_e are the variance and correlation length of the residuals, e, respectively. Plotted in Fig. 5 are the ECV (crosses) and GCV (solid line) functions. The correlation length of the best-fitting GCV function is 400 km (identical to that of GEOID96), but the variance is $(18.2 \text{ cm})^2$. This differs from the $(9.5 \text{ cm})^2$ variance for GEOID96. The similarity of correlation length makes sense, as the correlation length is very strongly connected to the size of the 48 separate GPS HARN adjustments (which is about 400 km, or the size of an average state). In order to determine the source of the higher variance, an ECV was computed from the residuals between G96SSS and the latest 6169 GPSBMs. That ECV had a correlation length of 400 km (as expected), and a variance of $(17.2 \text{ cm})^2$. This clearly confirms the higher variance as being related to the new GPSBMs and not gravimetric geoid changes. In fact, the higher variance was found to be due primarily to systematic biases in a few state HARNs that have been completed since 1996. Before proceeding to the collocation solution, it is important to discuss the source of this increased variance in more detail.

5.3 State-by-state biases

One important difference between the GPSBMs of 1996 and those of 1999 was the addition of new HARNs

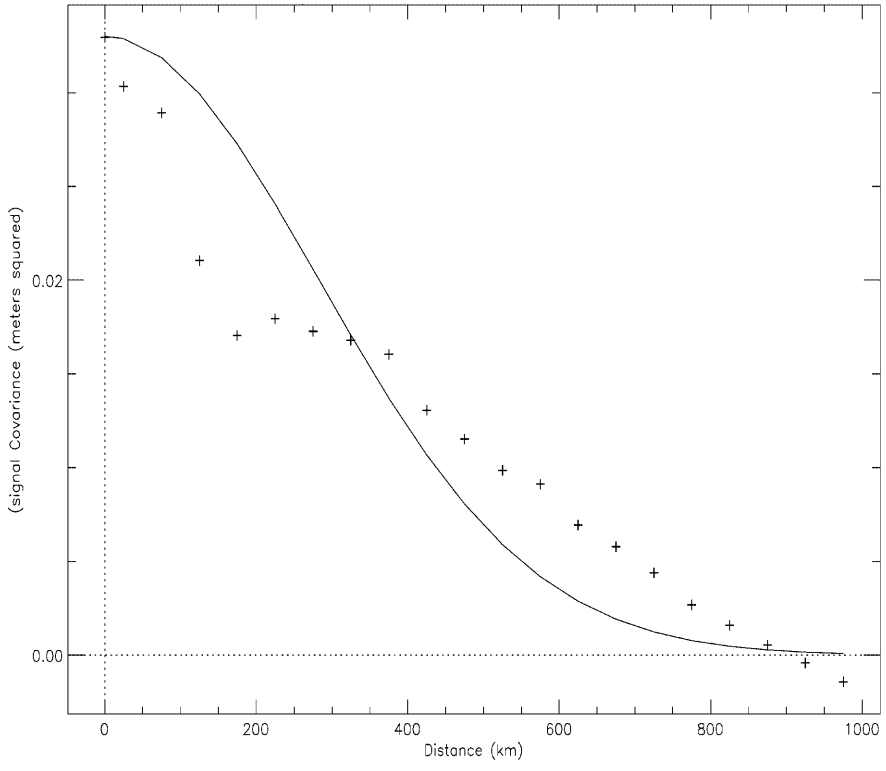

Fig. 5. Empirical covariance function (*crosses*) and best-fit Gaussian covariance function (*solid line*) implied by centered, detrended G99SSS/GPSBM residuals

(mostly in the central US), as well as the re-adjustment of certain areas (such as New England). What became more obvious with the larger 1999 data set was the existence of state-wide biases in many individual HARNs, due to the 'quasi-independent' nature of each HARN. To help identify state-by-state biases (which may contribute to the 0.15-ppm trend), the national average residual (+51.7 cm) was removed from the entire set of 6169 residuals, e, and the statistics of remaining residuals were investigated on a state-by-state basis. This is presented in Table 8, which shows that certain states and groups of states have residuals which differ from the national average by decimeters. Because the features of the geoid generally do not follow state boundaries, and because the NAVD 88 level network was not adjusted on a state-by-state bias, the most logical explanation for these state-by-state biases seems to be in the HARNs themselves. Each state's HARN is adjusted in a quasi-independent manner, with only a few ties to neighboring states. While theoretically these ties to neighboring states should force a cohesion from one HARN to another, this is clearly not the case in a few examples where two adjoining states have biases differing by over 10 cm, even though the standard deviation of residuals is on the order of a few centimeters (Illinois/Indiana, Florida/Georgia, Ohio/Michigan, etc). Table 8 leads to some inherent conclusions about the *precision* of the GPS surveys versus their *accuracy*. For example, in New Jersey there is only a 3.4-cm standard deviation of e over all 219 points, indicating high precision in the geoid, GPS, and leveling. Yet, the state-wide average e value is −23.5 cm from the national average, possibly indicating lower accuracy in the HARN adjustment. This is not a well defined rule, however. For example, in Washington and Oregon the formal error estimates on the HARN are 1 cm, yet the standard deviation of e is on the 14–16-cm level. This is caused by a large *systematic* east–west tilt in e across these two states (36 cm east–west or 0.65 ppm at an azimuth of 250°). A similar, though larger (42 cm east–west or 0.84 ppm at an azimuth of 238°), tilt existed in 1996 when G96SSS was compared to the 1996 GPSBMs.

The reason for a consistently tilted east–west residual field in the PNW is difficult to determine, since most of the information in this region changed between 1996 and 1999. There were new GPS heights observed and adjusted, a new gravimetric geoid model, and even a new NAD 83/ITRF transformation, all of which changed heights in Washington and Oregon. There is a general change of the overall slope of the geoid (0.8 ppm at an azimuth of 275°) between G96SSS and G99SSS. However, at the same time, there is a 0.24-ppm (at 25° azimuth) change between the 1996 e values and the 1999 e values, but this still leaves the overall east–west trend in the e field. This discrepancy of magnitude and direction of the overall tilt is accounted for, of course, by the large changes in reported ellipsoid heights (in the HARNs) in these two states, from 1996 to 1999 (see Fig. 2). Efforts are underway to identify the source of this tilt, but none of leveling, geoid, or GPS stands out as the definitive source.

What is most distressing about Table 8 are the two largest clusters: New England states ($\phi = 43°$N, $\lambda = 288°$E) into a large negatively biased area and PNW states ($42° \leq \phi \leq 49°$N, $235° \leq \lambda \leq 242°$E) into a positively biased area. Although altimetry is known to cause near-shore geoid tilts (Smith 1997), these clusters of large biases do not extend fully along the coasts. For example, North Carolina, South Carolina, and Georgia do not suffer the same biases as New England (and down to Virginia). Similarly, California does not suffer the same bias as the PNW. This again points toward state-by-state GPS adjustments as a likely component of this error.

One should be careful, however, not to blame GPS for all of the biases seen in Table 8. As noted, there are certainly correlations between the biases in some neighbor-

Table 8. State-by-state residuals after removal of national average (cm)

State	No. of points	Average	σ
Massachusetts	15	−48.0	7.7
Vermont	262	−41.3	6.9
New Hampshire	13	−40.7	3.4
Connecticut	1	−37.9	–
Rhode Island	1	−37.0	–
Maine	38	−33.0	5.7
New York	59	−28.9	9.9
New Jersey	219	−23.5	3.4
Virginia	102	−23.3	4.3
West Virginia	20	−21.6	8.4
Delaware	24	−19.4	3.7
District of Columbia	7	−18.6	3.6
Maryland	287	−18.0	4.2
Florida	482	−17.0	15.1
Pennsylvania	27	−16.7	6.2
Idaho	71	−12.6	6.8
Texas	280	−11.8	10.2
North Carolina	112	−10.5	8.9
Kentucky	89	−8.3	7.7
Utah	22	−8.2	7.0
Mississippi	68	−8.1	5.5
Nevada	34	−7.7	11.2
Arizona	102	−6.8	10.3
South Carolina	172	−5.8	6.7
New Mexico	50	−4.7	12.3
Alabama	161	−4.0	4.0
Tennessee	17	−4.0	7.0
Ohio	227	−3.9	4.6
Georgia	85	−0.9	7.7
California	434	0.3	13.1
Arkansas	24	0.6	3.7
Missouri	37	0.9	5.0
Kansas	55	1.9	4.6
Oklahoma	57	3.3	6.3
Nebraska	128	3.9	9.7
Wyoming	67	5.1	10.1
Louisiana	149	5.5	11.7
Indiana	97	6.0	8.2
Montana	128	8.0	17.3
Colorado	377	11.0	8.3
Iowa	61	11.2	8.8
Michigan	276	11.7	10.7
South Dakota	160	22.1	6.2
Illinois	112	22.6	8.8
Minnesota	603	30.2	5.8
Washington	163	30.8	14.7
Wisconsin	52	31.6	7.4
Oregon	114	37.9	16.7
North Dakota	27	40.2	4.0

ing states (Massachusetts, Vermont, New Hampshire, Connecticut, Rhode Island, Maine, New York, and New Jersey are one group; Washington and Oregon are another; other correlated values are also noticeable). It is already known that a correlation between state-by-state GPS adjustments might occur, as each HARN is 'quasi-independent', not truly independent, of its neighbors. However, correlations amongst neighboring states might also indicate an erroneous feature in the geoid, spanning multiple states (as in mountainous states such as Washington and Oregon, although the lack of a large positive bias in Idaho confuses this issue). Note also that, in general, the biases exhibit a noticeable east–west trend (western states have negative biases, eastern states have positive biases). This may be indicative of a tilt in the NAVD 88 level network. For the GPS-derived ellipsoid heights used in GEOID99, the formal accuracies of the GPS on an adjustment-by-adjustment basis 'seldom exceed' 10 cm [Vorhauer and Milbert (NGS), personal communication]. To summarize: GPS systematic errors contribute to the state-by-state biases but they are not necessarily the sole contributors.

5.4 Computation of GEOID99

In a manner similar to that of Smith and Milbert (1999), it was necessary to predict residuals $\hat{s}$ on a 30-arc-minute grid, using LS collocation with noise (Moritz 1980, pp. 102–106; Smith and Milbert 1999)

$$\hat{s} = C_{sl}[C_{ll} + c_{nn}]^{-1} l$$

Where (matrix sizes given in parantheses):

- $\hat{s}$ predicted residuals, e on a grid; "signal"(9729 × 1)
- C_{sl} variance-covariance matrix between residuals, e, at GPSBM locations and grid nodes (9729 × 6169)
- C_{ll} variance-covariance martix between residuals, e, at GPSBM locations (6169 × 6169)
- C_{nm} variance-covariance martix of random noise in the residuals, e, at GPSBM locations (6169 × 6169)
- l centered, detrended residuals, e (6169 × 1)

(11)

The 'noise' matrix, C_{nn}, is assumed diagonal with a single variance

$$C_{nn} = \sigma_0^2 i \tag{12}$$

This is the simplest solution, but a more formal solution would be to use a full C_{nn} matrix based on the combined formal noise estimates of GPS, leveling, and the gravimetric geoid. Unfortunately, no formal estimates of gravimetric geoid noise were computed at this time, and variance–covariance matrices in computing the leveled NAVD 88 heights are not readily accessible in the NGS archives. The GPS noise matrices are somewhat accessible from the state-by-state FBNVC adjustments, but without the leveling and geoid components a full C_{nn} matrix cannot be built. Efforts are underway at NGS to begin building a more accurate C_{nn} matrix, but they are in the preliminary stages. The elements of C_{ll} and C_{sl} were computed using the GCV of Eq. (10), where the variance and correlation length were $(18.2\text{ cm})^2$ and 400 km respectively. The iteration of σ_0^2 was performed as per Smith and Milbert (1999) to $\sigma_0^2 = (4.6\text{ cm})^2$. Then Eq. (11) was used to compute the predicted residuals on a 30-arc-minute grid. This grid is shown in Fig. 6, which is directly comparable to Fig. 5 of Smith and Milbert (1999).

The tilt, bias, transformation between ITRF96 and NAD 83, and LSC grid (Fig. 6) are next combined into a conversion surface (not shown). This surface is removed from G99SSS to minimize the differences between the predicted geoid values and those anticipated based upon the GPSBM data. The resulting hybrid model, GEOID99, incorporates all signals that can be modeled for intermediate to short wavelengths from the above error assessments, along with the long-wavelength signal in G99SSS. A color image of GEOID99 is available on the NGS geoid web page at http://www.ngs.noaa.gov/GEOID.

The difference between the hybrid models GEOID99 and GEOID96 is presented in Fig. 7. Note that in Fig. 7 the larger differences between G99SSS and G96SSS (Fig. 4) have been reduced due to the long-wavelength influence over the hybrid models that the GPSBMs exert.

GEOID99 was then compared to the same GPSBM data used above to determine the amount of improvement, and to gain a sense of how much noise was left in the residuals after the collocation process. New residuals, ε, are formed by the following equation:

$$\varepsilon = N_{99} - (h_{83} - H_{88}) \tag{13}$$

where N_{99} are the GEOID99 geoid undulations, ε are the adjusted, final residuals, and h_{83} are the GPS-derived ellipsoid heights in the NAD 83(86) reference frame. H_{88} is the same as H in Eq. (9) (NAVD 88 Helmert orthometric heights). For ε, the bias and tilt are zero. The ε values are representative of the errors in the observed data (GPS, geoid, and leveling combined). An ECV, based on ε, is computed by collecting ε into 'bins' of 1 km. The nature of this ECV seems to have two components: first a Gaussian spike ($\sigma_\varepsilon^2 = 4.6^2\text{ cm}^2$) is seen, but then a much smaller covariance, $\sigma_{\varepsilon 1,\varepsilon 2}$, is seen at the 2.5–3.5-cm level, decorrelating around 25 km. A GCV is fitted to this correlated error and shows a variance of $(2.5\text{ cm})^2$. Both the ECV and GCV are plotted in Fig. 8 (as crosses and solid line respectively).

6 Error analysis of GEOID99

As with previously released NGS geoid models, no formal accuracy estimates were computed for GEOID99 or G99SSS. This is due to many factors which complicate the process of error propagation (multiple data sources, unknown error correlations, using FFT for TC computation, and the Stokes integral). The computation of the gravimetric residual co-geoid undulations from residual Faye gravity anomalies was done through a 1-D FFT representation of the spherical Stokes integral (with ellipsoidal corrections), which inherently contains no formal accuracy estimation.

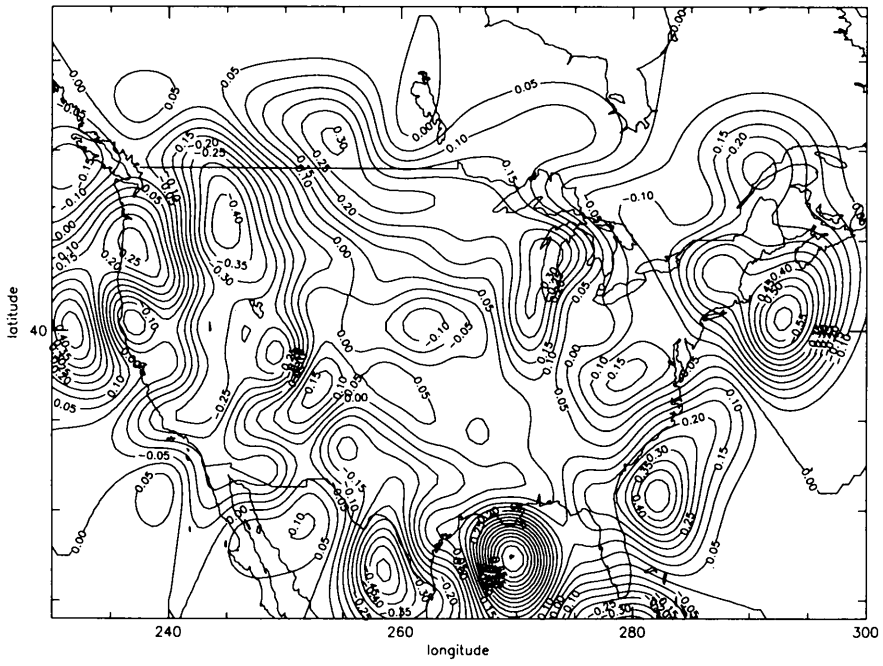

Fig. 6. Regional systematic trends of centered, detrended G99SSS/GPSBM residuals, as implied by LS collocation (C.I. = 5 cm)

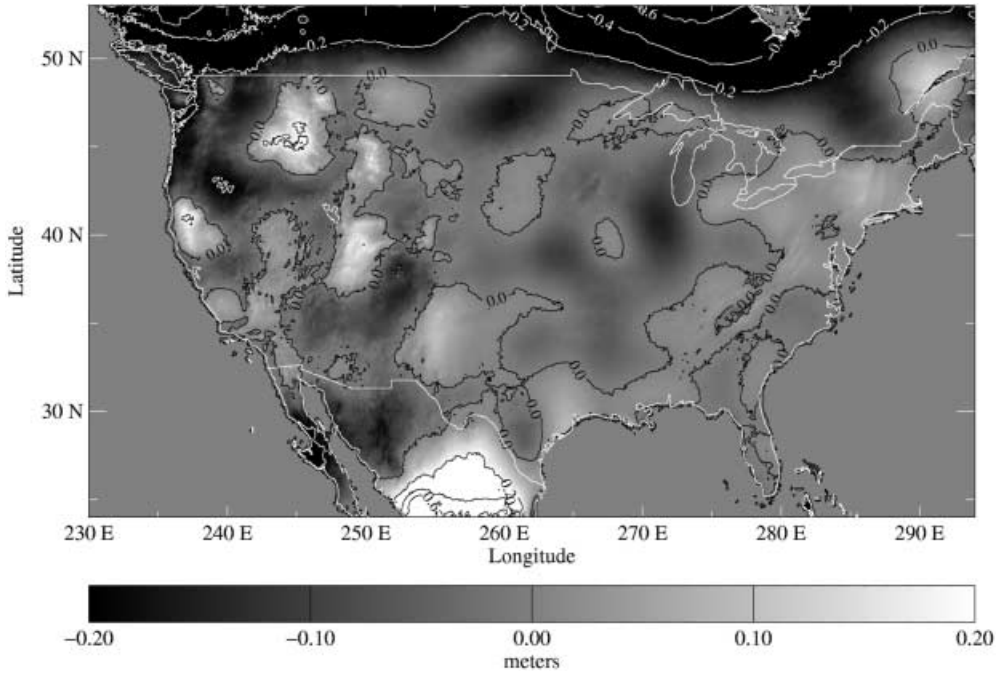

Fig. 7. Differences between GEOID99 and GEOID96

However, in the US the GPSBM data set has a fairly homogenous spatial distribution. While these data are used to control long-wavelength errors in the geoid model, they also provide an accuracy check. It is found, nationwide, that GEOID99 was able to reproduce GPS/leveling-derived geoid undulations at the ± 4.6-cm level. The sources of this disagreement are the error in GPS heights and geoid and leveling errors. Separation of the errors is difficult, but preliminary analysis indicates that 2.0–2.5 cm of the error is geoid error.

In 1993, Milbert (NGS, personal communication) performed some Monte Carlo estimates of the geoid error and found that the propagation of anomaly error into geoid error was bowl-shaped, leaving small (sub-centimeter) errors in the center of the country and large (>10 cm) errors in the oceans. This situation has changed somewhat with the inclusion of satellite altimetry, and numerous data and computational improvements since 1993, however.

Still, on a national average, it is possible to estimate the error one can expect from performing GPS/geoid leveling (acquiring differential 'GPS-derived orthometric heights') by examining the empirical covariance function (C_ε) implied by the residual between GEOID99 and GPSBMs, which was shown in Fig. 8. Assume the desired target is an orthometric height difference (ΔH^*),

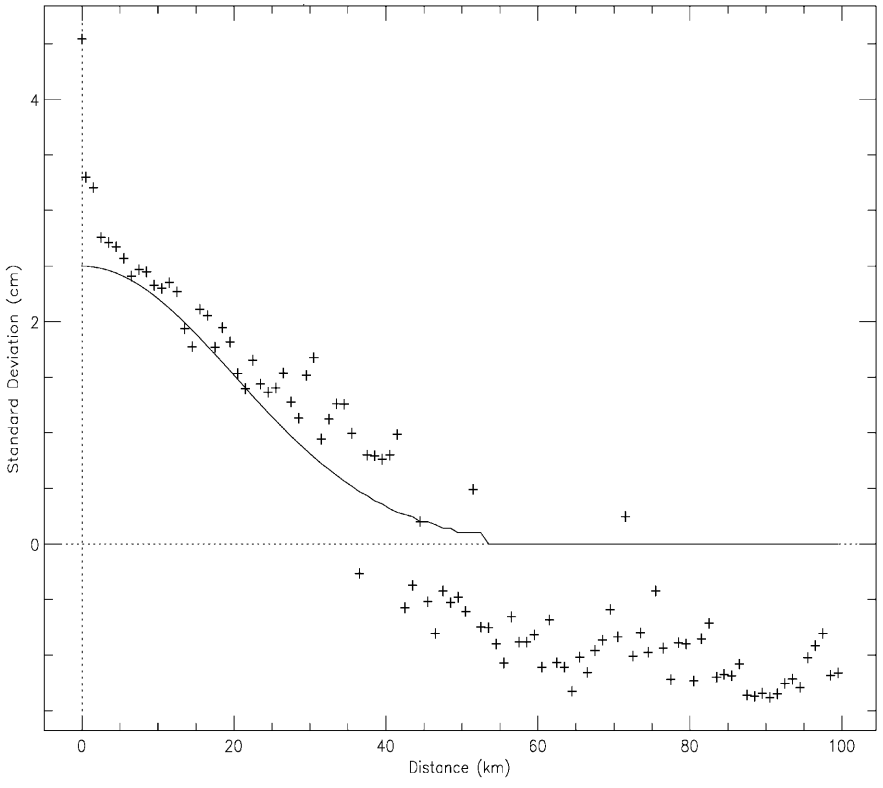

Fig. 8. Empirical covariance function (*crosses*) and best-fit (to correlated error) Gaussian covariance function (*solid line*) implied by GEOID99/GPSBM residuals

obtained through a combination of GPS and a geoid model (H^* is used to distinguish a GPS-derived orthometric height from a spirit-leveled orthometric height, H)

$$\Delta H^* = (H_1^* - H_2^*) = (h_1 - N_1) - (h_2 - N_2) \tag{14}$$

where h_1 and h_2 are GPS-derived ellipsoid heights at points 1 and 2, and N_1 and N_2 are hybrid geoid model undulations at points 1 and 2. The error variance in that differential height can be computed from simple error propagation. If one assumes that h and N each have a single variance, which is reasonable in small areas and if the GPS surveys are performed similarly at two points, then the equation is as follows:

$$\sigma^2_{\Delta H^*} = (2\sigma_h^2 - 2\sigma_{h_1,h_2}) + (2\sigma_N^2 - 2\sigma_{N_1,N_2}) \tag{15}$$

Recall that Fig. 8 has both the variance and co-variances of residuals, ε. These two pieces of information may be used to write the variance of a difference in residuals as

$$\sigma^2_{\Delta\varepsilon} = 2\sigma_\varepsilon^2 - 2\sigma_{\varepsilon_1,\varepsilon_2} \tag{16}$$

which expands to

$$\sigma^2_{\Delta\varepsilon} = (2\sigma_N^2 - 2\sigma_{N_1,N_2}) + (2\sigma_h^2 - 2\sigma_{h_1,h_2}) + (2\sigma_H^2 - 2\sigma_{H_1,H_2}) \tag{17}$$

If it is assumed that leveling is errorless (or at least negligible, relative to GPS and geoid errors) in a local area, such as 25 km or less, then Eqs. (15) and (17) may be set equal, and a model for the variance of a differential GPS-derived orthometric height is obtained as follows:

$$\sigma^2_{\Delta H^*} = 2\sigma_\varepsilon^2 - 2\sigma_{\varepsilon_1,\varepsilon_2} \tag{18}$$

Both σ_ε^2 and $\sigma_{\varepsilon 1,\varepsilon 2}$ are available from Fig. 8. Using the empirical covariance function of Fig. 8, the variance of residuals is $(4.6\text{ cm})^2$ and the co-variances can be inferred for distances (ψ_{ij}) from 1 up to 100 km. This presumes that the surveyor is doing similar-quality GPS work as that used for the GPSBM data set. There are formal accuracy estimates for each HARN adjustment, and in fact for each point (too numerous to mention here), but as a general description of the range of errors in all the HARNs, one can use this statement: "... between 1 and 10 cm vertical accuracy, depending on the age of the HARN, plus any systematic errors inherent in tying GPS to the older surveys like the eastern strain network" (D. Milbert [NGS], personal communication). If so, then one can compute the variance (and thus the standard deviation) expected in differential orthometric heights over short distances (based on *single ties* – that is, the a-priori error estimate of differential GPS-derived orthometric height errors between two points not in an LS-adjustment procedure) through Eq. (18). Using this method, errors in GPS-derived orthometric heights were computed for the GEOID96 model (Smith and Milbert 1999, Fig. 7) and also for GEOID99 (from Fig. 8). These errors are also respectively shown as lines A (solid circles) and B (plusses) in Fig. 9.

Note that for GEOID99 (line B), even at the shortest distances (0.5 km), there is over 4 cm of differential orthometric height error, which rises to a constant of about 6 cm at 40 km and greater. This is expected, as closer points have a higher correlation than distant points. Still, it means that even for short distances, GPS-derived orthometric heights are not comparable in accuracy to

traditional leveling. However, the situation is improving, as can be seen by the clear 2-cm improvement between GEOID96 and GEOID99 for all level line lengths, due to both an improved gravimetric geoid and improved GPS-derived ellipsoid heights in the GPSBM set.

In order to determine if the cause of the improvement between GEOID96 (line A) and GEOID99 (line B) was more dependent upon improved GPS or an improved gravimetric geoid, an experimental hybrid geoid 'GEOID96_99BM' was created. This was a hybrid geoid built from G96SSS and the 6169 GPSBMs of 1999. [In the collocation solution, the variance and correlation length of the GCV were $(17.2\text{ cm})^2$ and 400 km respectively, and the final absolute agreement between GEOID96_99BM and the 6169 GPSBMs was ± 5.1 cm.] The accuracy of differential GPS-derived orthometric heights from this experimental model is shown in Fig. 9 as line C (asterisks). Line C falls mostly in the middle of lines A and B, although it lies closer to line B for lines shorter than 20 km. This indicates that the improvement from GEOID96 to GEOID99 is due equally to the improvement in the gravimetric geoid signal as well as improved GPS precision (with a slightly higher dependence on GPS improvement at lines shorter than 20 km).

It is important to note, however, that the GEOID99 model was built using a single covariance function which was tailored to fit only the national average values of e. One could argue that a covariance function should be tailored to reflect the different nature of the GPS, leveling, and geoid in various parts of the country. There are some good reasons to consider this possibility. For example, the σ_ε^2 in Washington, Oregon, and Wisconsin (the three states with the 'best' GPS-derived ellipsoid heights available) is $(5.2\text{ cm})^2$, $(5.7\text{ cm})^2$, and $(5.6\text{ cm})^2$ respectively, all of which are larger than the $(4.6\text{ cm})^2$ national value! This is a clear indication that the accurate GPS in those three states are not being used to their full potential, and that the national covariance function [Eq. (10)] is not properly tailored to account for these good GPS data. In order to test this hypothesis, a separate covariance function was built using Eq. (10), but tailored to the GPSBMs in those three states [there were 27, 77, and 27 points with 1 cm (1σ) GPS heights in the states of Washington, Oregon, and Wisconsin respectively]. In this case the initial variance, σ_e^2, was $(12.0\text{ cm})^2$ and the correlation length remained somewhat large, being 180 km, which meant the generated trend surface was still fairly smooth. An experimental hybrid geoid ('G99_TAILORED') was built for these three states, using this tailored covariance function and an iterated value of σ_0^2 of $(3.5\text{ cm})^2$, and the final agreement in those three states was significantly improved over that of GEOID99. In Washington, Oregon, and Wisconsin the σ_ε^2 dropped to $(3.8\text{ cm})^2$, $(3.1\text{ cm})^2$, and $(3.3\text{ cm})^2$ respectively. The final variance–covariance function, C_ε, of this special three-state experiment is plotted in Fig. 10. Note that spacing of points forced 'bins' to be collected every 5 km and not every 1 km (as in Fig. 8), thus the points in Fig. 10 are more sparse than those in Fig. 8.

Using this three-state final covariance function, an estimate of differential GPS-derived orthometric height error ($\sigma_{\Delta H^*}$) was computed, as before, and is plotted as line D (diamonds) in Fig. 9. What this line indicates is how well *single-tie* differential GPS-derived orthometric heights could be achieved in states with 1-cm (1σ) GPS and a hybrid geoid tailored specifically to that data.

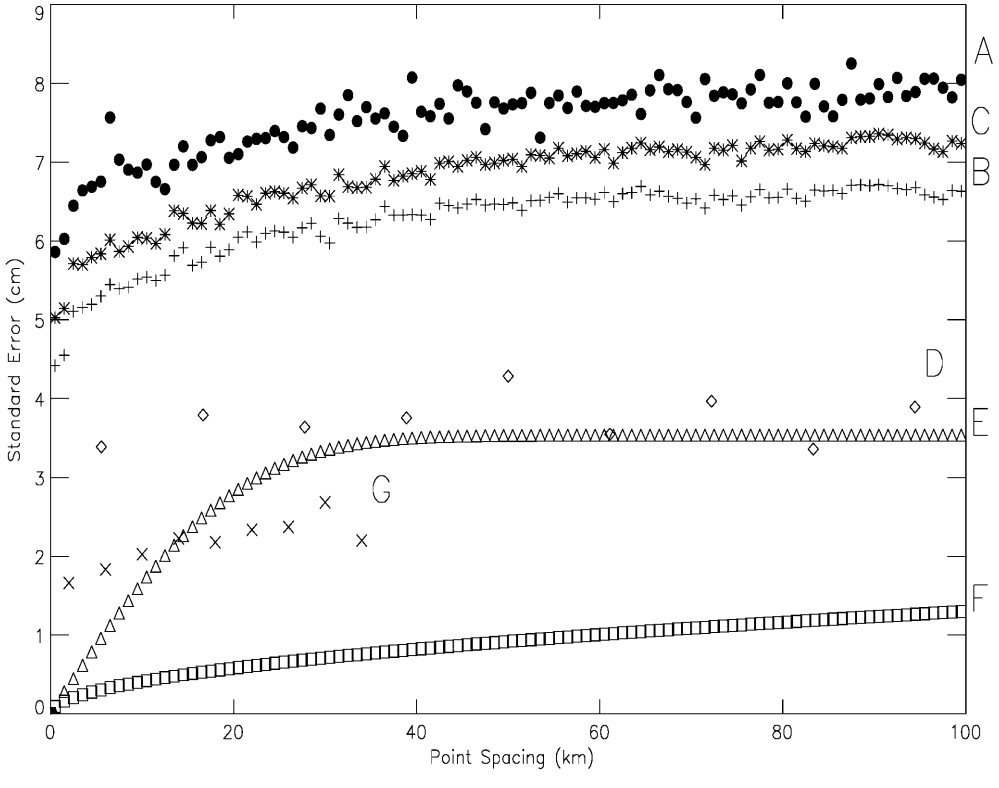

Fig. 9. Empirically derived differential orthometric height error for (A) GEOID96, (B) GEOID99, (C) GEOID96_99BM, (D) LSQ solutions in Washington, Oregon, and Wisconsin, using a tailored covariance function and 1-cm (1σ) GPS heights, (E) Gaussian covariance function of Fig. 8, (F) second-order, class II spirit leveling and (G) Baltimore County project

Because these error estimates are based on a single tie between neighboring points, and not on multiple ties in an LS adjustment, it is important to note that the error estimates shown in Fig. 9 may be driven down *much* further by the use of multiple-station ties in a 1-D vertical adjustment (Milbert 1991), as well as performing surveys in areas where the geoid error is smaller than that of Washington, Oregon, and Wisconsin.

In investigating the Washington, Oregon, Wisconsin issue, it is useful to examine the behavior of GEOID96_99BM in these three states so that one may quantify the improvements in the gravimetric geoids from 1996 to 1999. As mentioned above, the variance of GEOID99 residuals in these three states is $(5.2\text{ cm})^2$, $(5.7\text{ cm})^2$, and $(5.6\text{ cm})^2$ respectively. The variance of GEOID96_99BM residuals for these states is $(7.2\text{ cm})^2$, $(7.4\text{ cm})^2$, and $(5.8\text{ cm})^2$ respectively. Note that GEOID99 is about 2 cm better (RMS) in Washington and Oregon, as compared to GEOID96_99BM, while there is very little change in Wisconsin. This is expected, since the switch from 30-arc-second TCs (GEOID96_99BM) to 3-arc-second TCs (GEOID99) is probably driving the 2-cm improvements in Washington and Oregon, while very little changed in the DEM or gravity data in Wisconsin between 1996 and 1999.

If this example is taken one step further, and it is assumed that GPS error is only Gaussian (white noise) and is removed entirely from ε, leaving only correlated geoid error (which might be approximated by the GCV, solid line in Fig. 8), then $\sigma_{\Delta H^*}$ decreases again, reaching a maximum of ± 3.5 cm over 40 km. This theoretical case is shown as line E (triangles) in Fig. 9. For completeness, it should be mentioned that NGS has established a strategic goal to "... develop the capability to obtain second-order, class II (FGCS standards) orthometric heights using GPS combined with a high resolution geoid model" (Lapine 1994, p. 15). Second-order, class II accuracy $\sigma_{\Delta H}$ (in mm) can be computed from the distance between points, ψ_{km} (in km), by (FGCC 1984)

$$\sigma_{\Delta H} = (1.3\text{mm}) \times \sqrt{\psi_{\text{km}}} \tag{19}$$

This function is plotted as line F (squares) in Fig. 9. Line F is a target accuracy, and not achievable using a single tie between points until GPS *and* geoid errors are significantly reduced.

As a final, positive note on the accuracy of GPS-derived orthometric heights, one may turn to the highly successful 'Baltimore county project' (Henning et al. 1998) in the east coast area of Baltimore, Maryland. In that project, the final phase was the computation of GPS-derived orthometric heights from GEOID96 and very precise GPS procedures. These results were recalculated using the GEOID99 model [Zilkoski (NGS), personal communication] in 1999, and the accuracy results are plotted as line G (marked with X) in Fig. 9. One can clearly see that the combination of very accurate GPS and a well-known geoid (as GEOID99 is in Baltimore county) can yield orthometric heights accurate to < 2 cm level for 10-km lines.

7 GEOID99 and G99SSS in comparison with other regional geoid models

One frequently used strategy for identifying geoid errors, and planning future computations, has been

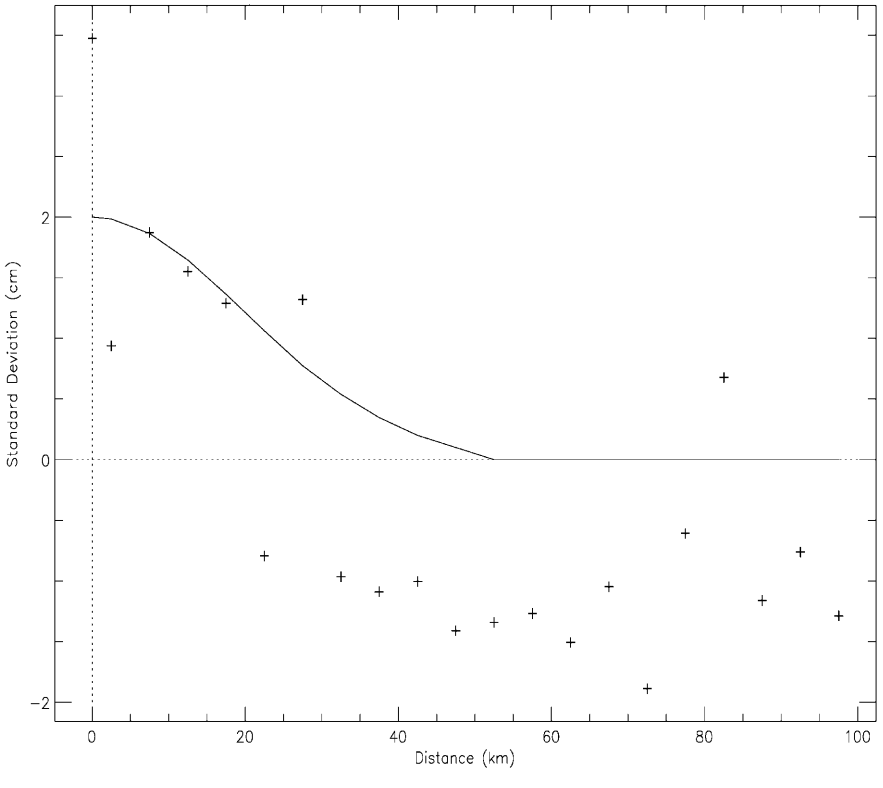

Fig. 10. Empirical covariance function (*crosses*) and best-fit (to correlated error) Gaussian covariance function (*solid line*) implied by GEOID99/GPSBM residuals in Washington, Oregon, and Wisconsin, using a tailored covariance function

comparison with other models. In the CONUS area, available non-NGS geoid models include the Canadian GSD95 (Véronneau 1997) and the NASA/NIMA EGM96 (Lemoine et al. 1998) model. Wherein the GSD95 model is definitely independent of G99SSS and GEOID99, it is not as obvious that the EGM96 model should be treated separately because it provides the reference gravity field for the computation of G99SSS and GEOID99.

The terrain and the high-density gravity signals used to develop G99SSS contain not only the high-frequency signal ommitted from the broader EGM96 gravity field, but also signal related to the errors in EGM96. These signals form at intermediate and longer wavelengths and are emphasized when the gravity data are converted to geoid undulations. This is even more so the case for GEOID99, where the same signal in G99SSS is further amplified by the GPSBM's (yet another independent data set). As such, comparisons to EGM96 for both GEOID99 and G99SSS are valid, because they incorporate independent information at a wavelengths that are registered by EGM96 and typify errors of commission as well as ommission. In addition, it will be useful to see what changes have occurred since the last NGS geoid models, GEOID96 and G96SSS (Smith and Milbert 1999).

7.1 Comparison of GEOID99 and G99SSS with GEOID96 and G96SSS

The GEOID99 model was planned to replace GEOID96 (Smith and Milbert 1999). With the improvements in data, methodology, and theory, as well as a statistically smaller residual relative to GPSBMs, GEOID99 was immediately approved as the replacement to GEOID96 at the NGS. Because the boundaries of GEOID99 (24°/58°N, 230°/300°E) extend beyond those of GEOID96 (24°/53°N, 230°/294°E), the comparison between the two will be limited to their common area. In order to accurately portray the difference due to grid spacing, GEOID96 was re-gridded to 1-arc-minute and a comparison to GEOID99 was made. The results are shown in Table 9.

The large reduction in σ (from G96SSS–G99SSS to GEOID96–GEOID99) in Table 9 indicates that while the two gravimetric models diverge significantly, the introduction of GPSBMs forces the two models toward a more common surface. Whether or not this is an advantage depends on the application. If the intent of geoid modeling is the pure pursuit of an equipotential surface, then the modification of the geoid through GPSBMs might indicate a biasing away from some expected 'truth'. However, Smith and Milbert (1999) show clear examples where the addition of GPSBM data actually reduces error in the gravimetric geoid in certain regions. Additionally, the geoid is a product as well as a scientific research project (see Vermeer 1998). That product has consumers (surveyors) who need it to convert GPS heights into leveled heights on the local vertical datum. From that viewpoint, the agreement between GEOID99 and GEOID96 is encouraging, and it can be interpreted that GPSBMs serve as a sort of centralizing focus for the hybrid geoid models.

One frequently cited justification for the national geoid model is the changing GPSBM data in NGSIDB. When new GPS and/or leveling is available, it effectively makes the last geoid model obsolete, in an *absolute* sense, as that model no longer reflects all available GPSBM data in the US. For surveyors working in local (< 400 km) areas, the long-wavelength changes in GPS heights will tend to average out, making the 'old' hybrid geoid still useful. In order to exemplify the problem of using an 'old' hybrid geoid with 'new' GPS on BM data, in an *absolute* sense, the GEOID96 model was compared to the 6169 GPSBMs used in creating GEOID99. Figure 11 shows the empirical covariance function, C_ε, from this comparison.

Note that in Fig. 11 the variance is $(6.5\text{ cm})^2$, and the correlated error is much higher than that seen in Fig. 8 (the GCV of Fig. 8 is plotted on Fig. 11 for reference). This indicates that GEOID96 is 'out of date' (in an absolute sense) relative to the currently available GPSBM data in the NGS database.

7.2 Comparison of GEOID99 and G99SSS with GSD95

The most currently available official geoid for Canada is the GSD95 model (Véronneau 1997). This is a purely gravimetric model, and a comparison of it to GEOID96 and G96SSS can be found in Smith and Milbert (1999). A similar comparison was made between GSD95 and G99SSS and GEOID99. It was expected that the −2.16-m difference between GSD95 and G96SSS would be reduced in G99SSS due to the use of 3-arc-second TCs. This was validated, and the discrepancy between the G99SSS and GSD95 is plotted in Fig. 12.

One can see by comparing Fig. 8 of Smith and Milbert (1999) to Fig. 12 of the present paper that the large 'pit' of disagreement in the PNW has been reduced in magnitude to −1.6 m (a 50-cm improvement in the agreement between Canadian and US models). However, there still remains a large east–west tilt between the US

Table 9. Differences between 1999 and 1996 geoid models (m)

Models	Minimum			Maximum			Average	σ
	Value	Latitude	Longitude	Value	Latitude	Longitude		
G99SSS – G96SSS	−3.6	24.08	283.12	+1.4	29.10	241.68	−0.507	±0.486
GEOID99 – GEOID96	−1.9	24.10	283.13	+2.0	24.07	253.98	−0.078	±0.194

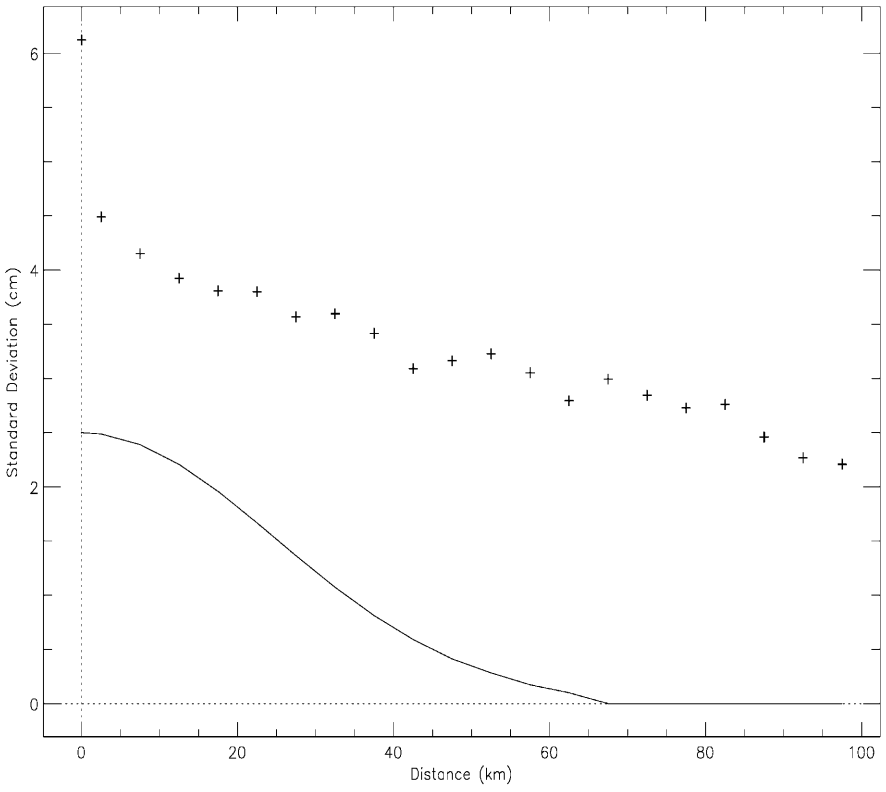

Fig. 11. Empirical covariance function (*crosses*) implied by residuals between GEOID96 and 1999 GPSBM set. Also shown is the 1996 Gaussian covariance function (*solid line*) which was best fit to the empirical covariance function of residuals between GEOID96 and the 1996 GPSBM set

and Canadian models. The tilt between GSD95 and G96SSS was 0.28 ppm at 67° azimuth (Smith and Milbert 1999). That has been reduced (but not eliminated) to 0.15 ppm at 82° azimuth. This represents a reduction in the overall east–west tilt from 125 cm down to 72 cm.

Because much of the GPSBM change in 1999 was in the northern part of the USA, it is interesting to see how these changes have affected the agreement between GEOID99 and GSD95. If one removes the −52-cm bias and the ITRF97/NAD83 transformation from GEOID99, then one is left with a geocentric hybrid model, which is designated G99BM. A similar comparison between G96BM and GSD95 is found in Smith and Milbert (1999). Figure 13 shows the differences between G99BM and GSD95.

The tilt between G99BM and GSD95 is 0.29 ppm at an azimuth of 121°. This is substantially different from the G96BM/GSD95 tilt (Smith and Milbert 1999). As such, it is inconclusive whether a tilt exists between GEOID99 and GPSBMs, or whether a tilt comes from GSD95. The two most likely sources of this tilt are the influence of a poor DEM in the Quebec region, and the extension of GEOID99 to 58°N, which is far removed from any GPSBMs in the USA. Considering the tilts seen in studying the Quebec DEM, it is possible that a remaining bias in the region is corrupting the northeast corner of the G99SSS model. Because there were no GPSBMs in Quebec (at the NGS), that corruption remains in the GEOID99 model. The recent acquisition of the Canadian Digital Elevation Data (CDED) data from Canada may alleviate this problem in the future. However, since GEOID99 is not built for use outside the US, the impact on US surveyors is minimal.

7.3 Comparison with EGM96

As with GEOID96, comparison of the most recent GPSBM data set is also made with a 15-arc-minute grid of undulations derived from EGM96 coefficients and correction coefficients. (Rapp 1992, 1997). The modified EGM96 model was regridded to a 1-arc-minute interval to compare with the results of the G99SSS model.

Color representations (not in this paper) of the differences between EGM96 and G99SSS were made and compared to the color images of EGM96/G96SSS differences (Smith and Milbert 1999, Fig. 10). A full representation of all these color images is available on the NGS web site (http://www.ngs.noaa.gov/GEOID). The values of EGM96 minus G99SSS range from −139 cm to +344 cm. These values average 9 cm with a ±34 cm standard deviation. (In the smaller area of G96SSS, these statistics have an average of 12 cm, minimum of −139 cm, maximum of 344 cm, and standard deviation of ±36 cm.) These numbers show an improved agreement between NGS and EGM96 from 1996 to 1999 (G96SSS/EGM96 residuals average 11.7 cm, after correcting for the 12-cm bias in G96SSS, with a standard deviation of ±39 cm). The most significant regional changes occurred in the PNW and the Gulf of Mexico. The reduced amplitudes in these regions probably reflect the incorporation of multi-band TC methods in the PNW and the use of KMS98 altimetry in the Gulf of Mexico.

The modified-EGM96 grid was also compared with the GPSBM data. The residuals averaged 46 cm with a standard deviation of ±40 cm, further emphasizing the

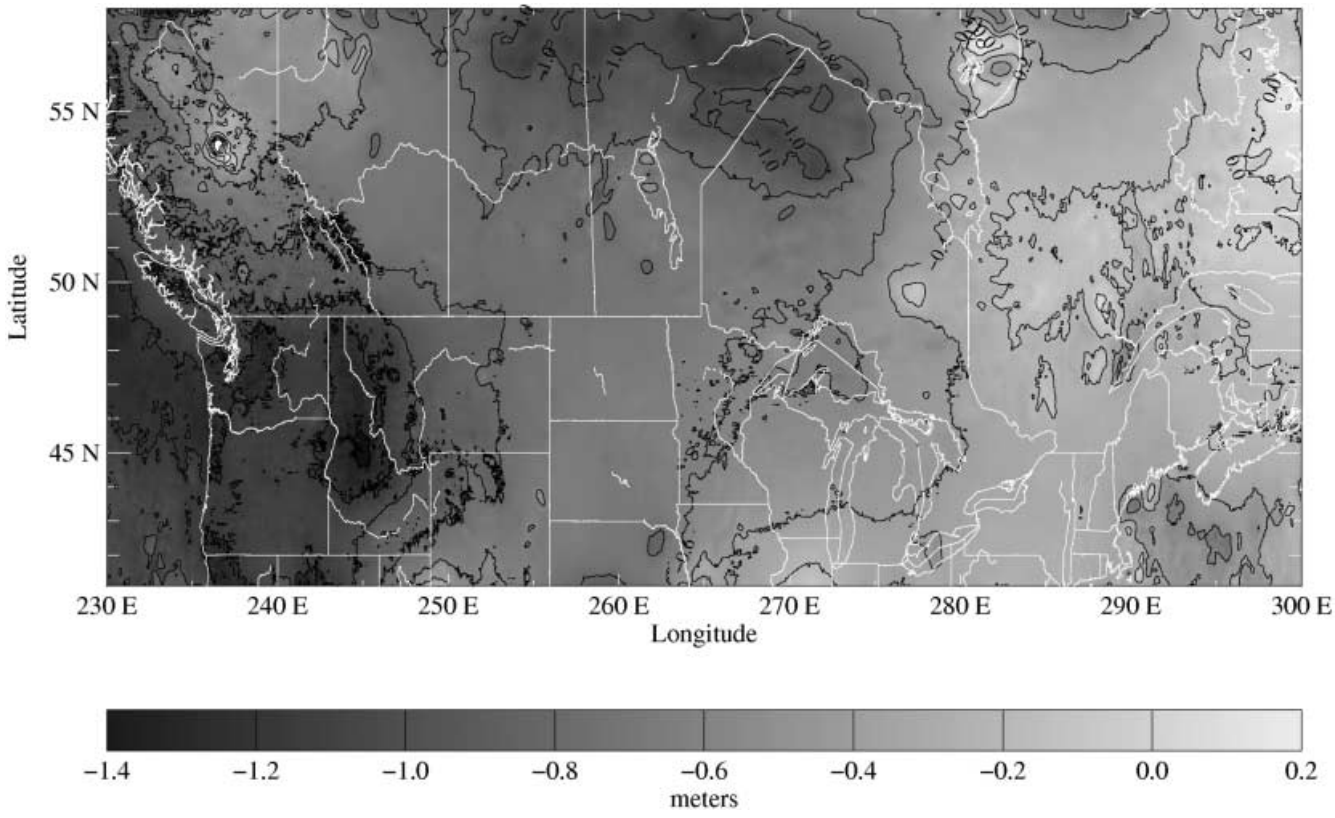

Fig. 12. Differences between G99SSS and the Canadian GSD95 geoid models (C.I. = 20 cm)

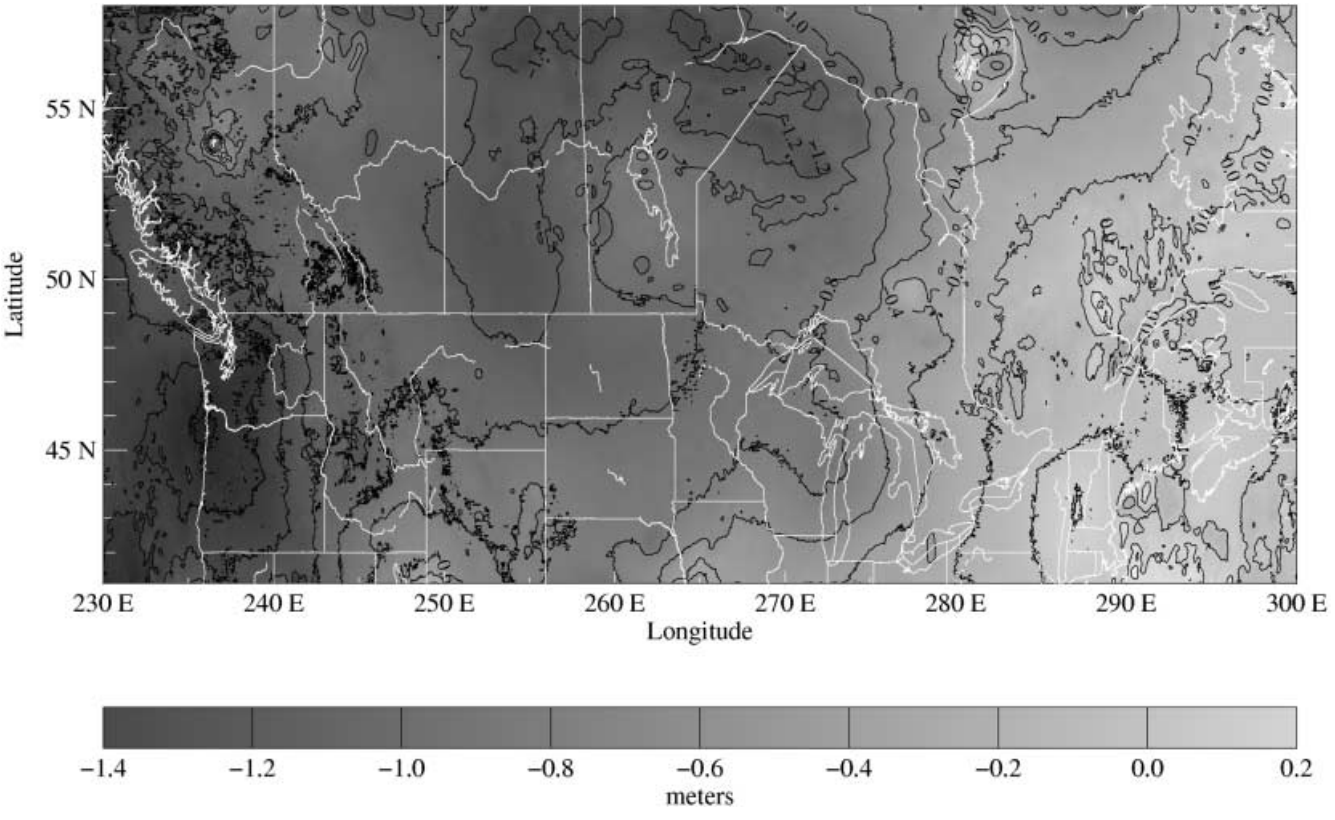

Fig. 13. Differences between G99BM and the Canadian GSD95 geoid models (C.I. = 5 cm)

significant high-frequency data loss when using EGM96 rather than a high-resolution geoid model.

8 DEFLEC99 computation

A deflection-of-the-vertical (DOV) model, DEFLEC99, was computed as a companion to the GEOID99 model. It is built to convert geodetic latitudes and longitudes in NAD 83 into astronomic latitudes and longitudes. The computation of DEFLEC99 (following the process developed for DEFLEC96 by Milbert (NGS), personal communication) begins by computing slopes of GEOID99 at the level of the geoid through the use of bi-cubic splines

$$\xi_g = -\frac{1}{R}\frac{\partial N}{\partial \phi}$$
$$\eta_g = -\frac{1}{R\cos\phi}\frac{\partial N}{\partial \lambda} \tag{20}$$

where

ξ_g N/S DOV at surface of genoid
η_g E/W DOV at surface of geoid
N GEOID99
ϕ NAD 83 latitude
λ NAD 83 longitude
R Mean earth radius

After computing the DOVs at the geoid, a correction ($d\Phi$ and $d\Lambda\cos\Phi$) for the curvature of the plumb line (between the geoid and surface of the Earth) was computed [Heiskanen and Moritz 1967, Eq. (5–32)]. Horizontal derivatives of topography (β_1 and β_2) were obtained from the mean 1-arc-minute DEM. The mean value of gravity along the plumb line (and subsequently its horizontal derivatives) was computed using the DEM and a grid of simple Bouguer anomalies with the simplified Prey reduction [Heiskanen and Moritz 1967, Eq. (4–24)]. Once the plumb-line curvature corrections are computed, the final surface deflections (which are used by surveyors) are obtained by

$$\xi_s = \xi_g + \delta\Phi$$
$$\eta_s = \eta_g + \delta\Lambda\cos\phi \tag{21}$$

where the subscripts s and g refer to the Earth's surface and geoid levels, respectively.

The GEOID99 DOVs were compared to a set of 3398 astro-geodetically determined deflections of the vertical (AGDOVs) in the NGSIDB. The geodetic coordinates of the AGDOVs refer to NAD 83, and the astronomic coordinates refer to the BTS-84 reference frame, rotated by 0.365 arc seconds in longitude to coordinate BTS-84 with NAD 83 (Schwarz 1989, pp. 83–84). A comparison was made between these astro-geodetic DOVs and the DOVs of both DEFLEC96 and DEFLEC99. The results are shown in Table 10.

As expected, Table 10 shows a slight improvement in the agreement with AGDOVs when one moves from DEFLEC96 to DEFLEC99. The high-resolution TCs used in DEFLEC99 in the PNW combined with the finer 1-arc-minute resolution of the computations clearly added new geoid (and thus deflection) information, and the second half of Table 10 clearly shows the amount of improvement in the PNW.

The source of the approximately 0.1-arc-second average residuals seen in Table 10 is harder to explain. Possible causes are a 0.5-ppm tilt in NAVD 88 in both the north–south and east–west directions. However, this translates to a 2.5-m east–west tilt and a 5.0-m north–south tilt. There is no evidence to support such large tilts, and in this paper as well as previous papers (Smith and Milbert 1999), there has been good evidence of little or no tilt in NAVD 88. What is more likely is a combination of possible systematic errors in the reduction of the AGDOVs and gravimetric (hybrid) DOVs, summing up to 0.1 arc seconds.

9 Future directions

While GEOID99 was definitely successful as a more accurate geoid than GEOID96 in relation to BMs, there are many research items that remain unaddressed. This is especially true if one considers the stated strategic goal (Sect. 6) of '... second order, class II leveling ...' with GPS and a geoid model. This goal effectively coincides with the frequently quoted target of a '1-cm geoid'. That is, the ability to convert GPS heights into leveled heights for any baseline length. To achieve this goal, many steps must be taken from all sides of this program.

Starting with the geoid itself, more rigorous theoretical solutions to and formulations of the fundamental boundary value problem of physical geodesy are needed. In fact, this problem itself is often posed in the spherical domain, when in fact it more accurately belongs in the ellipsoidal (Fei and Sideris 2000). At the NGS, plans are currently underway to replace the existing geoid software with more rigorous computations. Included in this are true Helmertization of the global terrain signal using non-planar coordinates, actual rock densities, and regularization techniques for downward continuation. In addition, the long-wavelength structure of the geoid will be more accurately controlled through the introduction of the GRACE, CHAMP, and GOCE satellite gravity missions.

Improved geoid theory will only be as good as the data used with it, and so a comprehensive plan for analyzing gravity and DEM data at the NGS is also in the planning stages. The difficulties with the Bahamas and Gulf of Mexico gravity data cause near-shore tilts in the geoid, requiring some solution (such as airborne gravity surveys). In addition, an expansion of the NGSDEM99 1-arc-second DEM is planned. This expansion should cover all of the CONUS by the end of 2003 and all other states and territories by 2004. In addition, a Memorandum of Understanding (MOU) between the NGS and GSD Canada has been signed, giving the NGS access to more accurate DEM data in Canada (hopefully solving the Quebec DEM problems).

Table 10. Statistics of residuals between 3398 astro-geodetic and gravimetric (hybrid) deflections of the vertical (arc seconds)

	No. of points	ξ (N/S)		η (E/W)	
		Average	σ	Average	σ
AGDOV – DEFLEC96 (National)	3398	0.11	±0.97	−0.13	±0.92
AGDOV – DEFLEC99 (National)	3398	0.13	±0.88	−0.16	±0.85
AGDOV – DEFLEC96 (PNW)	464	0.09	±1.04	−0.22	±1.20
AGDOV – DEFLEC99 (PNW)	464	0.16	±0.83	−0.25	±1.09

From the GPS side, the FBNVC project is proceeding with a projected end date sometime in 2003. At that time, the NGS will begin a continent-wide re-adjustment of the NAD 83 reference frame in cooperation with Canada, Mexico and perhaps Caribbean and Central American nations. When this occurs, state-by-state biases in the GPS are expected to be eliminated, leaving one coherent set of GPS heights at the 1-cm (1-σ) level.

One often-overlooked issue has been errors in the NAVD 88 level network. However, increased accuracy in both the geoid and GPS has led many NGS researchers to believe that errors in the leveling may now actually be detectable with GPS and the geoid. In the next few years, a detailed examination of the leveling in a few areas will begin. This may help, for example, to finally solve the reason for a tilted residual field between h, H, and N in Washington and Oregon.

Finally, the combination of the gravimetric geoid with GPS and leveling through collocation will be modified. In the past, a homogenous, isotropic Gaussian covariance function [Eq. (10)] has been used. It was seen in this paper that such a function does not truly model the differences in GPS accuracy on a state-by-state basis. As such, new covariance functions (non-homogenous, perhaps even non-isotropic) will be investigated and possibly applied to the creation of the next hybrid geoid model.

Finally, the changing nature of the NGS, GPSBM data means that even GEOID99 will be somewhat out of date within perhaps one year. As such, annual geoid models are being considered at the NGS. It is most likely that such models will build upon similar gravimetric geoids, but with new conversion surfaces built through new GPSBMs.

10 Conclusions

Two new, high-resolution geoid models for the USA and its territories have been computed at the NGS. These models are the gravimetric G99SSS model and the hybrid GEOID99 model, both covering the area 24° to 58°N latitude and 230° to 300°E longitude for the CONUS. Gravimetric geoids were also produced for Alaska, Hawaii, and Puerto Rico and the American Virgin Islands. In addition, DOV models were produced for all of these areas. The G99SSS and GEOID99 models replace the G96SSS and GEOID96 models of the NGS.

There were significant improvements in geoid computations between 1996 and 1999. On the gravimetric side, a new 1-arc-second DEM was introduced for the PNW, eliminating tens of milliGals of TC error in that mountainous region. In addition, new multi-band applications of 2-D FFT TC computations were used to eliminate north–south systematic errors due to meridian convergence. To further reduce north–south tilts, the ellipsoidal corrections of Fei and Sideris (2000) were applied to the gravimetric geoid. Further improvements include correction of mis-registration errors in the TOPO30 DEM, elimination of DEM biases in Quebec, and introduction of the KMS98 altimetry-based gravity anomalies.

Also, since 1996, the number of good GPS heights on leveled bench marks has more than doubled. Besides just densifying points, the quality of the GPS data has improved. In fact, the three most recent states added to the NGSIDB were part of the FBNVC – a project to re-observe each state's HARN network with the intent of producing 1-cm (1-σ) GPS heights. This improved GPS quality led directly to an improvement in the hybrid geoid accuracy. However, the state-by-state nature of the HARN adjustments has left state-wide biases in many states. This problem will not be alleviated until consistency in GPS heights is achieved in 2002 or 2003 with the planned NGS re-adjustment of the NAD 83 network.

GEOID99 was created in September 1999 based on the G99SSS gravimetric geoid and 6169 GPS heights on leveled bench marks. It has the ability to replicate NAVD 88 Helmert orthometric heights from GPS at the ±4.6-cm level, in an absolute sense. This is an improvement over the ±5.5-cm level for GEOID96. In addition, GEOID99 is shown to better approximate differential leveling than GEOID96 by nearly 2 cm at all line lengths when using only two points ('single tie'). Statistics for this improvement when using points in a network adjustment are not currently available. However, very large strides in improving both GPS and geoid theory must still be made if GPS-derived orthometric heights are ever to approach the formal accuracy of traditional spirit leveling.

Acknowledgements. The number of people who contributed to the success of the GEOID99 project is immense. First off, thanks to Dr. Carlos Aiken (University of Texas at Dallas) for contributing over 100 000 new gravity measurements to the NGS gravity database. And special thanks to Zhiling Fei and Dr. Michael Sideris for making the ellipsoidal correction computations for this project. Thanks to the following organizations that contributed data to the NGS: NIMA, NASA, USGS, Geomatics Canada, and the Danish National Cadastre.

References

Andersen OB, Knudsen P (1998) Global marine gravity field from the ERS-1 and Geosat geodetic mission altimetry. J Geophys Res 103(C4): 8129–8137

Bodnar AN (1990) National Geodetic Reference System statewide upgrade policy. Tech papers of ACSM–ASPRS American Congress on Surveying and Mapping and American Society of Photogrammetry and Remote Sensing Fall Convention, 5–10 November, 1990: A-71–82

Burša M (1995) Report of Special Commission SC3, Fundamental constants. Presented at the 21st General Assembly of the International Association of Geodesy, Boulder, CO, 2–14 July

Dewhurst WT (1990) NADCON: the application of minimum curvature-derived surfaces in the transformation of positional data from the North American Datum of 1927 to the North American Datum of 1983. NOAA (National Oceanic and Atmospheric Administration) tech memo NOS NGS-50, Rockville, MD

Doyle DR (1993) High accuracy reference networks development, adjustment and coordinate transformation. Presented at the ACSM/ASPRS Annual Convention, New Orleans, LA, 15–18 February

Federal Geodetic Control Committee (1984) Standards and specifications for geodetic control networks. Federal Geodetic Control Committee, Silver Spring, MD

Fei ZL, Sideris MG (2000) A new method for computing the ellipsoidal correction for Stokes's formula. J Geod 74(2): 223–231

Flynn KC (1998) The last HARN: completing the national high accuracy reference network. ACSM Bull 175(Sep/Oct): 23–27

Frakes S (1999) Surveying the Federal base network. ACSM Bull 182: 28–29

Haagmans R, de Min E, van Gelderen M (1993) Fast evaluation of convolution integrals on the sphere using 1-D FFT, and a comparison with existing methods for Stokes' integral. Manuscr Geod 18(5): 227–241

Hastings DA, Dunbar PK (1999) Global Land One-kilometer Base Elevation (GLOBE), version 1.0: key to geophysical records documentation, nr 34. National Geophysical Data Center, Boulder, CO

Heiskanen WA, Moritz H (1967) Physical geodesy. WH Freeman, San Francisco, CA

Henning WE, Carlson EE, Zilkoski DB (1998) Baltimore County, Maryland, NAVD 88 GPS-derived orthometric height project. Surv Land Info Syst 58(2): 97–113

Kirby JF, Featherstone WE (1999) Terrain correcting Australian gravity observations using the national digital elevation model and the fast Fourier transform. Aust J Earth Sci 46: 555–562

Kotsakis C, Sideris MG (1999) The high-frequency structure of the gravity field in Canada. Presented at the 25th annual meeting of the Canadian Geophysical Union, Banff, Alberta

Lapine LA (1994) National Geodetic Survey: its mission, vision and strategic goals. Internal rep, Coast and Geodetic Survey, Silver Spring, MD

Lemoine FG, Kenyon SC, Factor JK, Trimmer RG, Pavlis NK, Chinn DS, Cox CM, Klosko SM, Lutchke SB, Torrence MH, Wang YM, Williamson RG, Pavlis EC, Rapp RH, Olson TR (1998) The development of the joint NASA GSFC and the National Imagery and Mapping Agency (NIMA) geopotential model EGM96. NASA tech publ 1998–206861. Greenbell, Maryland, USA

Milbert DG (1991) Computing GPS-derived orthometric heights with the GEOID90 geoid height model. Tech papers 1991 ACSM–ASPRS Fall Convention, Atlanta, 28 October–1 November. Am Congr Surv Map, Washington, DC, pp A46–55

Milbert DG (1998) Documentation for the GPS benchmark data set of 23-July-98, IGeS Bull 8, Int Geoid Service, Milan, December, pp 29–42

Moritz H (1980) Advanced physical geodesy. Herbert Wichmann, Karlsruhe

Parks W, Milbert DG (1995) A geoid height model for San Diego County, California, to test the effect of densifying gravity measurements on accuracy of GPS-derived orthometric heights. Surv Land Info Syst 55(1): 21–38

Rapp RH (1992) Computation and accuracy of global geoid undulation models. Proc Sixth Int Geodetic Symp Satellite Positioning, The Ohio State University, Columbus, 17–20 March, pp 865–872

Rapp RH (1997) Use of potential coefficient models for geoid undulation determinations using a spherical harmonic representation of the height anomaly/geoid undulation difference. J Geod 71(5): 282–289

Row III LW, Kozleski MW (1991) A microcomputer 30-second point topography database for the conterminous United States. User manual, version 1.0. National Geophysical Data Center, Boulder, CO

Schwarz CR (ed) (1989) North American datum of 1983. NOAA Professional Paper NOS 2, Rockville MD

Sillard P, Altamimi Z, Boucher C (1998) The ITRF96 realization and its associated velocity field. Geophys Res Lett 25(17): 3223–3226

Smith DA (1997) The impact of different satellite altimeter gravity anomaly data sets on geoid height models. Presented at the Fall meeting of the American Geophysical Union, San Francisco, CA

Smith DA (1998) There is no such thing as "the" EGM96 geoid: subtle points on the use of a global geopotential model. IGeS Bull 8, International Geoid Service, Milan, December, pp 17–28

Smith DA, Milbert DG (1999) The GEOID96 high resolution geoid height model for the United States. J Geod 73(5): 219–236

Smith DA, Roman DR (1999) Documentation for the GPS benchmark data set of August 27, 1999. Online NGS document: http://www.ngs.noaa.gov/GEOID/GPSonBM99/gpsbmdoc99.html

Smith DA, Roman DR (in press) A new high resolution DEM for the Northwest United States. Surv Land Info Syst

Smith DA, Small HJ (1999) The CARIB97 high resolution geoid height model for the Caribbean Sea. J Geod 73(1): 1–9

Smith DA, Sartori M, Milbert DG (2001) Preliminary investigations toward and improved geoid model in Florida. Surv Land Info Syst 60(2): 109–116

Snay RA (1999) Using the HTDP software to transform spatial coordinates across time and between reference frames. Surv Land Info Syst 59(1): 15–25

Strang Van Hees G (1990) Stokes formula using fast Fourier techniques. Manuscr Geod 15(4): 235–239

Strange WE, Love JD (1991) High accuracy reference networks; a national perspective. Presented at the American Society of Civil Engineers Specialty Conference – Transportation Applications of GPS Positioning Strategy, Sacramento, CA, 18–21 September

United States Geological Survey (1997) GTOPO30, Global 30 arc second elevation data set. WWW distribution at: http://edcwww.cr.usgs.gov/landdaac/gtopo30/gopo30.html

Vermeer M (1998) The geoid as a product. Proc Second Continental Workshop on the Geoid in Europe, 10–14 March, 1998. Springer-Verlag, Berlin Heidelberg New York

Véronneau M (1997) The GSD95 geoid model for Canada Eds. Segawa J, Fujimoto H, Okubo S. Proc Int Symp Gravity, Geoid, and Marine Geodesy (GRAGEOMAR 1996), Tokyo, 30 September–5 October 1996. Springer, Berlin, Heidelberg New York, pp 573–580

Zilkoski D, Richards J, Young G (1992) Results of the general adjustment of the North American Vertical Datum of 1988. Surv Land Info Syst 52(3): 133–149